REPORT DO

AD-A236 808

READ INSTRUCTIONS BEFORE COMPLETING FORM

1. REPORT NUMBER
21

RECIPIENT'S CATALOG NUMBER

4. TITLE (and Subtitle)
Effect of Annealing on the Ferroelectric Behavior of Nylon 7 and Nylon 11

TYPE OF REPORT & PERIOD COVERED
Technical

6. PERFORMING ORG. REPORT NUMBER

7. AUTHOR(s)
J.W. Lee, Y. Takase, B.A. Newman and J.I. Scheinbeim

8. CONTRACT OR GRANT NUMBER(s)
N00014-88-K-0122

9. PERFORMING ORGANIZATION NAME AND ADDRESS
Dept. of Mechanics and Materials Science
College of Engineering, Rutgers University
Piscataway, New Jersey 08855-0909

10. PROGRAM ELEMENT, PROJECT, TASK AREA & WORK UNIT NUMBERS

11. CONTROLLING OFFICE NAME AND ADDRESS
Dr. Joanne Milliken
Office of Naval Research
Arlington, VA 22217-5000

12. REPORT DATE
May 1991

13. NUMBER OF PAGES
33

14. MONITORING AGENCY NAME & ADDRESS(if different from Controlling Office)

15. SECURITY CLASS. (of this report)
UNCLASSIFIED

15a. DECLASSIFICATION/DOWNGRADING SCHEDULE

16. DISTRIBUTION STATEMENT (of this Report)
Approved for public release; distribution unlimited. Reproduction in whole or in part is permitted for any purpose of the United States Government.

17. DISTRIBUTION STATEMENT (of the abstract entered in Block 20, if different from Report)

18. SUPPLEMENTARY NOTES
Published, J. Polym. Sci., Polym. Phys. Ed.

19. KEY WORDS (Continue on reverse side if necessary and identify by block number)

20. ABSTRACT (Continue on reverse side if necessary and identify by block number)
We have recently discovered that melt quenched and cold-drawn nylon 11 films exhibit very clear ferroelectric hysteresis behavior. In the present study, a remanent polarization as high as 86 mC/m^2 has been found in nylon 7 samples; this is significantly higher than that usually observed in poly(vinylidene fluoride) films. The effect of annealing on the electric displacement, D, vs. electric field, E, characteristics of both nylon 11 and 7 films have been studied and show an increased coercive field (62 to 115 MV/m for nylon 11 and 79 to 97 MV/m for
OVER

DD FORM 1 JAN 73 1473

UNCLASSIFIED
SECURITY CLASSIFICATION OF THIS PAGE (When Data Entered)

91 6 12 048

91-01969

nylon 7) and a decreased remanent polarization (51 to 17.3 mC/m^2 for nylon 11 and 86 to 70.5 mC/m^2 for nylon 7) with increasing annealing temperature, 25°C to 145°C.

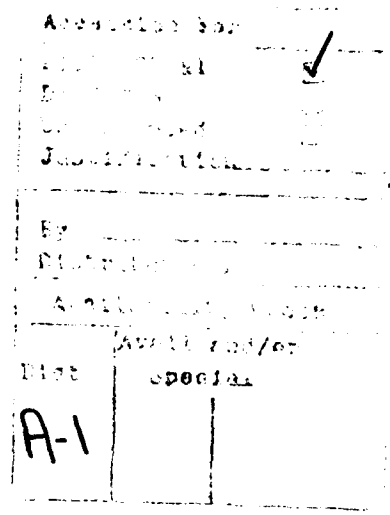

OFFICE OF NAVAL RESEARCH

Contract N00014-88-K-0122

Technical Report No. 21

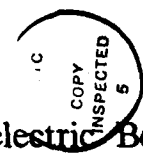

Effect of Annealing on the Ferroelectric Behavior of Nylon 7 and Nylon 11

by

J.W. Lee, Y. Takase, B.A. Newman and J.I. Scheinbeim

Prepared for Publication in

J. Polym. Sci., Polym. Phys. Ed.

Department of Mechanics and Materials Science
College of Engineering
Rutgers University
Piscataway, NJ 08855-0909

May 1991

Effect of annealing on the Ferroelectric Behavior of Nylon 7 and Nylon 11

J. W. Lee, Y. Takase, B. A. Newman, and J. I. Scheinbeim

Department of Mechanics and Materials Science, College of Engineering, Rutgers University, Piscataway, New Jersey 08854

Abstract

We have recently discovered that melt quenched and cold-drawn nylon 11 films exhibit very clear ferroelectric hysteresis behavior. In the present study, a remanent polarization as high as 86 mC/m^2 has been found in nylon 7 samples; this is significantly higher than that usually observed in poly(vinylidene fluoride) films. The effect of annealing on the electric displacement, D, vs electric field, E, characteristics of both nylon 11 and 7 films have been studied and show an increased coercive field (62 to 115 MV/m for nylon 11 and 79 to 97 MV/m for nylon 7) and a decreased remanent polarization (51 to 17.3 mC/m^2 for nylon 11 and 86 to 70.5 mC/m^2 for nylon 7) with increasing annealing temperature, 25°C to 145°C.

INTRODUCTION

Extensive studies using X-ray diffraction[1,2,3] and Infrared spectroscopy[4,5] have been carried out by many researchers in order to understand the ferroelectric behavior of poly(vinylidene fluoride) (PVF_2). In addition, many studies of electric field induced dipole reversal phenomena, in terms of electric displacement, have been reported.[6,7] From this evidence, scientists now believe that the piezoelectric and pyroelectric activity in PVF_2 results from the phase I crystals with preferred dipole orientation along the poling field direction. Many other polymers, under appropriate poling conditions, have been found to be piezoelectric[8] but it is somewhat surprising that only PVF_2 and its copolymers have been shown to exhibit the electric displacement, D, vs electric field, E, hysteresis behavior, typical of ferroelectric materials.

In a series of recent papers[9-11], Newman, Scheinbeim and others have reported that by using appropriate poling conditions and sample microstructure, relatively large piezoelectric strain constants ($d_{31} \approx 3$ pC/N) can be obtained for some odd nylons. In addition, an unique study of the piezoelectric response from an initially heavily plasticized, then crystallized during poling, nylon 11 film showed an even higher piezoelectric strain constant ($d_{31} \approx 7.1$ pC/N)[12]. Preliminary experiments carried out in our laboratory have also shown that initially quenched and then cold-drawn nylon 11 can exhibit clear ferroelectric hysteresis loops

at room temperature and below[13], the remanent polarization obtained from the D vs E characteristics being 56 mC/m^2.

In order to better understand the ferroelectric nature of the odd nylons, and as part of a study to determine the optimal sample preparation conditions for enhancing remanent polarization and piezoelectric coefficients in odd nylons, we decided to study the effects of annealing melt quenched nylon 11 and nylon 7 films before poling.

EXPERIMENTAL

The nylon films used in this study were prepared by melting the nylon powder between aluminum foils in a hot press at 210°C and 240°C for nylon 11 and nylon 7, respectively. Then, the molten films were quenched by placing them into an ice bath. The quenched films were then uniaxially stretched to a draw ratio of 3:1 at room temperature.

The annealing process was performed under vacuum at 55°C, 70°C, 85°C, 115°C, 145°C, and 185°C for two hours. The samples were held at a fixed length during the annealing procedure to prevent shrinkage and significant loss of chain orientation.

Aluminum electrodes (≈ 12.5 mm^2) were evaporated on both sides of the films after annealing. The evaporation process was carried out carefully in order to avoid overheating the samples. Then, the samples were dried and stored under high vacuum conditions until they were poled in order to limit water absorption.

The current density, J, and electric displacement, D, versus electric field, E, hysteresis characteristics were determined at room temperature using a silicone oil bath. A triangular shaped electric field pulse with a maximum amplitude of 150 MV/m, and a period of 640 seconds was applied to both types of nylon samples. However, because of conduction problems, the nylon 7 films were pre-treated by applying a static electric field of 170 MV/m for one hour before application of the triangular field. This was done to field-sweep out most of the conductive species. The dielectric constant, piezoelectric strain and stress constants, and the elastic modulus were measured at room temperature at 3.3 Hz after poling, using a Rheolograph Solid^{R} (Toyoseiki, Japan).

Wide angle X-ray diffraction scans, in both transmission and reflection modes, were obtained using nickel filtered CuKα radiation.

RESULTS

J and D VS E HYSTERESIS CHARACTERISTICS

Figure 1 and Figure 2 show the measured current density versus electric field after the annealing treatment for nylon 11 and nylon 7, respectively. The J vs E characteristics for both types of nylon samples show clear switching current peaks. From the peak positions, the apparent coercive fields are 62 and 79 MV/m at 25°C for the as-stretched nylon 11 and nylon 7 samples, respectively. The difference in coercive field between the two nylon samples indicates that the (polar) amide groups in nylon 7

are more difficult to rotate under field than those of nylon 11 for similar preparation histories.

Furthermore, significant dc conduction shows up in all the test samples, even when the samples are carefully prepared and dried. Therefore, it is useful to use a corrected current density to obtain the D vs E hysteresis figures. This was discussed in a previous publication.[13]

In both types of nylon samples, the current density peak becomes broader and the peak height decreases after annealing. Finally, the peak totally disappears as the annealing temperature reaches 185°C. In addition, the coercive field (peak position) shifts to higher electric fields with increasing annealing temperature. This indicates that dipole reorientation becomes more and more difficult with increasing annealing temperature. From the shape of the measured current density, it appears that maximum polarization cannot be obtained using a maximum applied field of 150 MV/m. However, in order to avoid significant numbers of sample breakdown, the maximum field was limited to 150 MV/m for both types of nylon samples. The D vs E hysteresis characteristics are obtained by integrating the corrected current density with respect to time. Figures 3 and 4 show the electric displacement vs electric field behavior for nylon 11 and nylon 7, respectively. In both figures, we can clearly see typical D vs E ferroelectric hysteresis loops and from intersections of the hysteresis loops with the D axis, the estimated remanent polarization is 51 and 86 mC/m^2 for the as-stretched nylon 11 and

nylon 7 samples, respectively. These large remanent polarization values are the first such observations in the odd nylons. The remanent polarization decreases as the annealing temperature increases and almost no remanent polarization can be observed when the annealing temperature reaches 185°C.

The coercive field and remanent polarization vs annealing temperature are presented in Figure 5 and Figure 6, respectively. Apparently, the coercive field increases and remanent polarization decreases with increasing annealing temperature in both nylon 7 and nylon 11. This indicates that well annealed and then poled samples undergo significantly less dipole reorientation in both types of nylons.

PIEZOELECTRIC AND DIELECTRIC MEASUREMENTS

Figures 7 to 10 show the elastic modulus, dielectric constant and piezoelectric strain and stress coefficients (d_{31} and e_{31}) versus annealing temperature, respectively. The elastic modulus of both nylons increases slightly with increasing annealing temperature and nylon 7 has a higher modulus than nylon 11 for all annealing conditions. A slight decrease in dielectric constant with increasing annealing temperature is seen in Figure 8 and the difference between the two nylons is small. The decrease in piezoelectric activity, d_{31} and e_{31}, with increasing annealing temperature is consistent with the decrease in remanent polarization shown in Figure 6.

X-RAY DIFFRACTION MEASUREMENTS

Figures 11 and 12 show the wide angle X-ray diffraction scans in reflection mode for nylon 11 and nylon 7, respectively, at different annealing temperatures. We observe that the X-ray diffraction scans of both types of nylon samples are similar in two respects. First, their crystallinity as measured by the area under the diffraction peak increases with increasing annealing temperature. Second, their peak position shifts to higher 2θ angles, which indicates closer lateral packing after annealing. Furthermore, the 2θ-value of the diffraction peak for as-stretched nylon 11 is smaller than that of as-stretched nylon 7. The 2θ-peak position for the two types of nylons become very close after the annealing treatment at 185°C (see Figure 15).

Figures 13 and 14 show the wide angle X-ray diffraction scans in transmission mode for nylon 11 and nylon 7, respectively. The diffraction peaks in transmission mode, more or less, remain at the same 2θ-value regardless of the annealing temperature, while the intensity change with annealing is much smaller than that observed in the reflection scan mode.

Figure 15 shows the 2θ-value (peak positions for both reflection and transmission modes) versus annealing temperature for both types of nylons. In the case of as-stretched nylon 11, due to the pseudo-hexagonal structure we cannot distinguish which planes are contributing to the diffraction peak observed in the X-ray reflection mode and which planes are contributing to the diffraction peak observed in the X-ray transmission mode. But,

apparently, we can distinguish the diffracting planes in the case of the as-stretched nylon 7 sample because the observed difference in the 2θ-values (difference in the peak position between reflection and transmission modes) is about 0.52° before annealing. In addition, very different changes are observed in the peak positions (2θ-values) with increasing annealing temperature between the reflection and transmission modes for both types of nylons, strongly indicates that some orientation exists in the samples. This orientation phenomenon will be discussed later.

DISCUSSION

Nylon 7 and nylon 11 are semicrystalline polymers possessing both crystalline and amorphous regions[14]. It is therefore important to determine which regions are responsible for the observed ferroelectric behavior. At this time, it appears very unlikely that the ferroelectric behavior originates in the amorphous regions. If we assume that nylon 12 has similar amorphous regions to those of nylon 11 or nylon 7 and if we also assume that the amorphous regions are ferroelectric, then we should find a comparable (or at least significant) dipolar reversal phenomenon for nylon 12 samples as well as for the nylon 11 and nylon 7 samples. However, we found no trace of ferroelectric behavior in any of the nylon 12 test samples which were prepared and poled under the same conditions as the nylon 11 samples. Also, from the sharp current density switching peaks

shown in Figures 1 and 2, it appears that the crystalline regions in both types of odd nylon samples are ferroelectric. If ferroelectric switching occurs in the amorphous regions, one might expect a broad switching current density peaks rather than the sharp peaks observed in the J vs E characteristics shown in Figures 1 and 2.

On the other hand, if we assume that the crystalline regions are ferroelectric, then one might expect that the higher the crystallinity the larger the ferroelectric response. This suggestion, apparently, is inconsistent with the annealing results, because the sample annealed at the highest annealing temperature (185°C) has the highest crystallinity and the lowest ferroelectric response. This result presents a rather complicated and puzzling feature of the ferroelectric nature of both types of odd nylons. However, if one carefully examines the X-ray diffraction results, one can provide an explanation as to how the annealing treatment affects the ferroelectric behavior of these nylons.

The significant shift of the observed 2θ-values and the large increases in diffracted intensity with increasing annealing temperature were only observed in the reflection modes but not in the transmission modes of the X-ray diffraction scans (see Figures 11 to 15). Furthermore, samples that were melt quenched but not drawn and then annealed did not exhibit the phenomenon as described above. These results indicate that a preferential orientation was developed during the drawing process. Similar

observation have also been discussed by Bonart[15] and Northolt[16]. Since only planes parallel to the film surface can contribute to the observed X-ray intensity in the reflection mode, it appears on the basis of the observed d-spacing for the annealed films compared with the d-spacing provided in the literature of odd nylons[17,18] that the hydrogen bonded sheets are approximately in the plane of the films. In other words, large rearrangements (closer packing) between the hydrogen bonded sheets were observed in the X-ray reflection scans after annealing. Once the orientation of the hydrogen bonded sheet structure is understood, the puzzling features can be interpreted in the following way. The as-stretched samples have the largest lateral spacing between sheets, which allows the amide groups to more easily rotate toward the field direction and to find a suitable hydrogen bonding partner. But after annealing, the d-spacings (4.21Å and 4.09Å for the as-stretched nylon 11 and nylon 7 films, respectively) between hydrogen bonded sheets becomes smaller and smaller (3.88Å and 3.87Å for nylon 11 and nylon 7 annealed at 185°C, respectively) until the amide groups can no longer rotate under the electric field. In other words, the activation energy needed to rearrange the well packed sheet structure is much higher than that possible to achieve with a maximum applied field of 150 MV/m. Therefore, the ferroelectric nature of these odd nylons disappears with increasing annealing temperature. A more detailed study of the crystal structure responsible for the observed ferroelectric behavior of the odd nylons is under way.

CONCLUSIONS

We have clearly established that nylon 11 and nylon 7 are ferroelectric polymers. Nylon 11 and nylon 7 exhibited their highest values of Pr, d_{31} and e_{31} for annealing temperatures below 50°C and below 115°C, respectively. The maximum values of Pr observed were 51 and 86 mC/m^2 for nylon 11 and nylon 7, respectively. The maximum values obtained for d_{31} were 2.3 and 1.8 pC/N for nylon 11 and nylon 7, respectively. The maximum values obtained for e_{31} were 6.4 and 7.1 mC/m^2 for nylon 11 and nylon 7, respectively. The results of the X-ray diffraction studies and the electrical measurements suggest three important features regarding the ferroelectric behavior of nylon 7 and nylon 11.

(1) Quenched and then cold-drawn and annealed nylon 7 and nylon 11 films show clear ferroelectric behavior over a large annealing temperature range.

(2) The ferroelectric behavior of nylon 7 and nylon 11 and the lack of observed ferroelectricity in nylon 12 clearly indicates that this phenomenon originates in the crystalline regions.

(3) The observed decrease in the ferroelectric behavior of nylon 7 and nylon 11 and the increase in apparent coercive field due to the annealing treatment can be interpreted in terms of a rearrangement of the hydrogen bonded sheet structure in these nylons, i. e. a significant decrease in spacing between hydrogen

bonded sheets after annealing which results in an increased difficulty for the amide groups to reorient with poling.

Finally, it should be pointed out that under similar sample preparation and appropriate poling conditions, lower order odd nylons (1,3,5) may exhibit even larger remanent polarizations.

ACKNOWLEDGMENT

This work was supported by DARPA and the office of Naval Research.

References

1. G. T. Davis, J. T. Mckinney, M. G. Broadhurst, and S. C. Roth, J. Appl. Phys. 49, 4998 (1978).
2. R. G. Kepler and R. A. Anderson, J. Appl. 49, 1232 (1978).
3. Takahashi and A. Odajima, Ferroelectrics, 32, 49 (1981).
4. D. Naegele and D. Y. Yoon, Appl. Phys. Lett. 33, 132 (1978).
5. F. J. Lu and S. L. Hsu, Polymer, 25, 1247 (1984).
6. M. Tamura, K. Ogasawara, N. Ono, and S. Hagiwara, J. Appl. Phys. 45, 3768 (1974).
7. T. Furukawa and M. Date, J. Appl. Phys. 54, 1540 (1983).
8. J. Mort, G. Pfister, Electronic Properties of Polymers, Wiley, New York, 1982, p. 140.
9. B. A. Newman, P. Chen, K. D. Pae, and J. I. Scheinbeim, J. Appl. Phys. 51, 5161 (1980).
10. J. I. Scheinbeim, J. Appl. Phys. 52, 5939 (1981).
11. S. C. Mathur, J. I. Scheinbeim, and B. A. Newman, J. Appl. Phys. 56, 2419 (1984).
12. J. I. Scheinbeim, S. C. Mathur, and B. A. Newman, J. Polym. Sci. (Polym. Phys. Edn.) 24, 1791 (1986).
13. J. W. Lee, Y. Takase, B. A. Newman, And J. I. Scheinbeim, accepted for publication, J. Polym. Sci. (1989).
14. M. I. Kohan, Nylon Plastics, Wiley, New York, 1973.
15. R. Bonart, Kolloid Z., 231, 438 (1969).
16. M. G. Northolt, J. Polym. Sci., part C, 38, 205 (1972).
17. W. P. Slichter, J. Polym. Sci., 36, 259 (1959).

18. A. Kawaguchi, T. Ikawa, Y. Fujiwara, M. Tabuchi, and K. Monobe, J. Macromol. Sci.-Phys., B20, 1 (1981).

Figure Captions

Figure 1 Annealing temperature dependence of the measured current density, J, as a function of electric field, E, when nylon 11 is subjected to a triangular electric field pulse with a maximum amplitude of 150 MV/m.

Figure 2 Annealing temperature dependence of the measured current density, J, as a function of electric field, E, when nylon 7 is subjected to a triangular electric field pulse with a maximum amplitude of 150 MV/m.

Figure 3 Annealing temperature dependence of the electric displacement, D, calculated from the data in Figure 1 as a function of electric field, E for nylon 11.

Figure 4 Annealing temperature dependence of the electric displacement, D, calculated from the data in Figure 2 as a function of electric field, E for nylon 7.

Figure 5 The coercive field (peak position in the J vs E curve) vs annealing temperature for nylon 11 and nylon 7.

Figure 6 The remanent polarization, Pr, vs annealing temperature for nylon 11 and nylon 7.

Figure 7 The elastic modules vs annealing temperature for nylon 11 and nylon 7 after poling.

Figure 8 The dielectric constant vs annealing temperature for nylon 11 and nylon 7 after poling.

Figure 9 The piezoelectric strain constant ,d_{31}, vs annealing temperature for nylon 11 and nylon 7 after poling.

Figure 10 The piezoelectric stress constant, e_{31}, vs annealing temperature for nylon 11 and nylon 7 after poling.

Figure 11 Annealing temperature dependence of the wide angle X-ray diffraction scans (reflection mode) for as-stretched nylon 11 film.

Figure 12 Annealing temperature dependence of the wide angle X-ray diffraction scans (reflection mode) for as-stretched nylon 7 film.

Figure 13 Annealing temperature dependence of the wide angle X-ray diffraction scans (transmission mode) for as stretched nylon 11 film. The as-stretched sample (25°C) has a larger half width than the annealed samples (115°C and 185°C).

Figure 14 Annealing temperature dependence of the wide angle X-

ray diffraction scans (transmission mode) for as-stretched nylon 7 film.

Figure 15 Annealing temperature dependence of the peak 2θ-value of wide angle X-ray diffraction scans (reflection and transmission mode) for as-stretched nylon 7 and nylon 11 films.

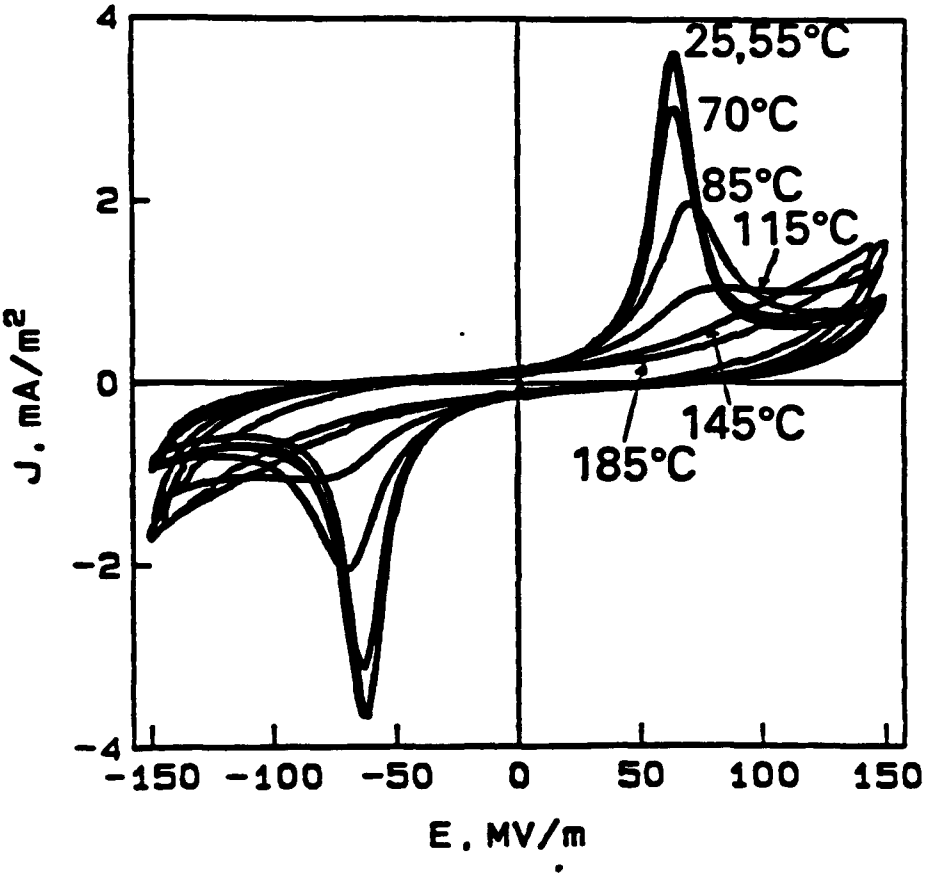
4
2
0
-2
-4
J, mA/m²
-150
-100
-50
0
50
100
150
E, MV/m
25,55°C
70°C
85°C
115°C
145°C
185°C

Fig. 1

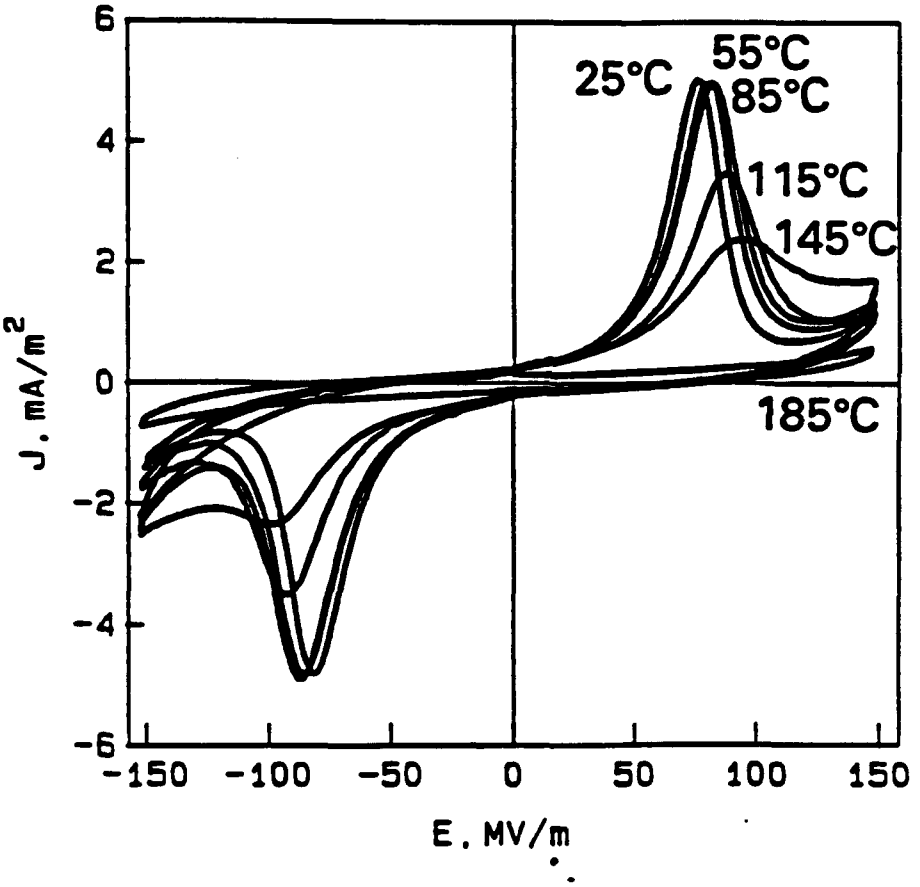
6
4
2
0
-2
-4
-6
-150
-100
-50
0
50
100
150
J, mA/m2
E, MV/m
25°C
55°C
85°C
115°C
145°C
185°C

Fig. 2

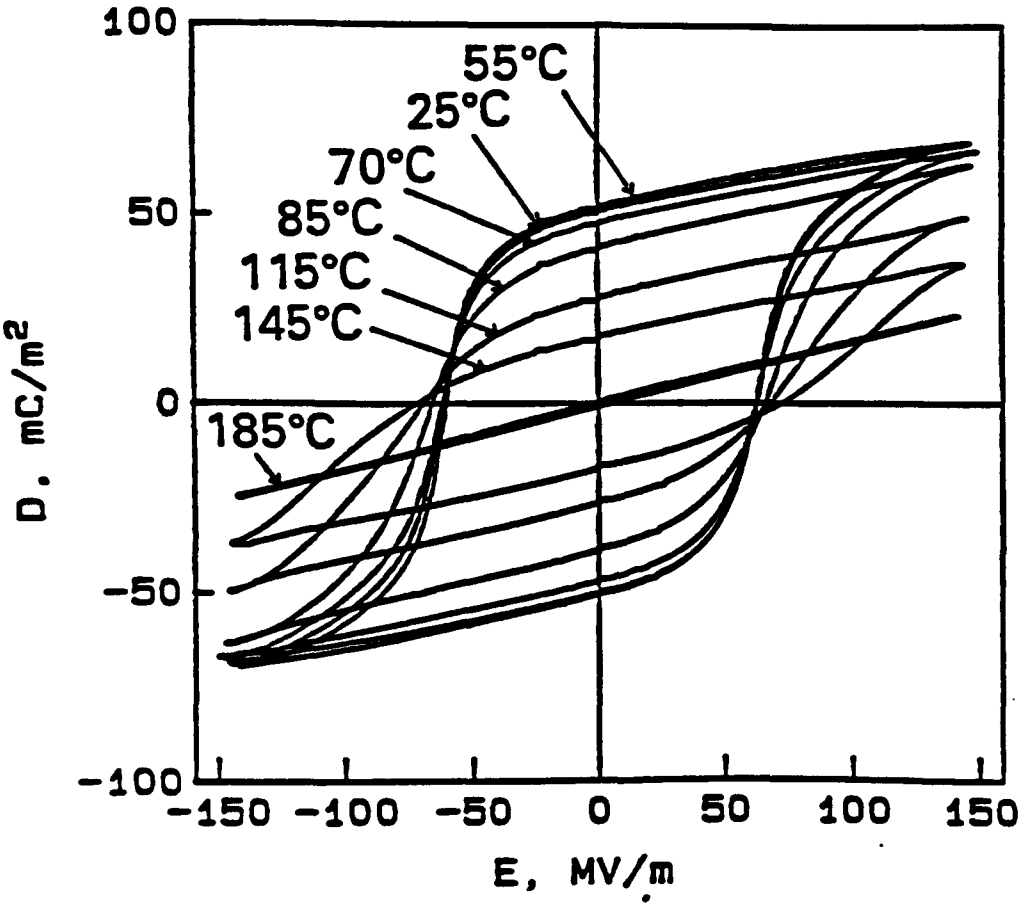
100
50
0
-50
-100
-150
-100
-50
0
50
100
150
55°C
25°C
70°C
85°C
115°C
145°C
185°C
D, mC/m²
E, MV/m

Fig. 3

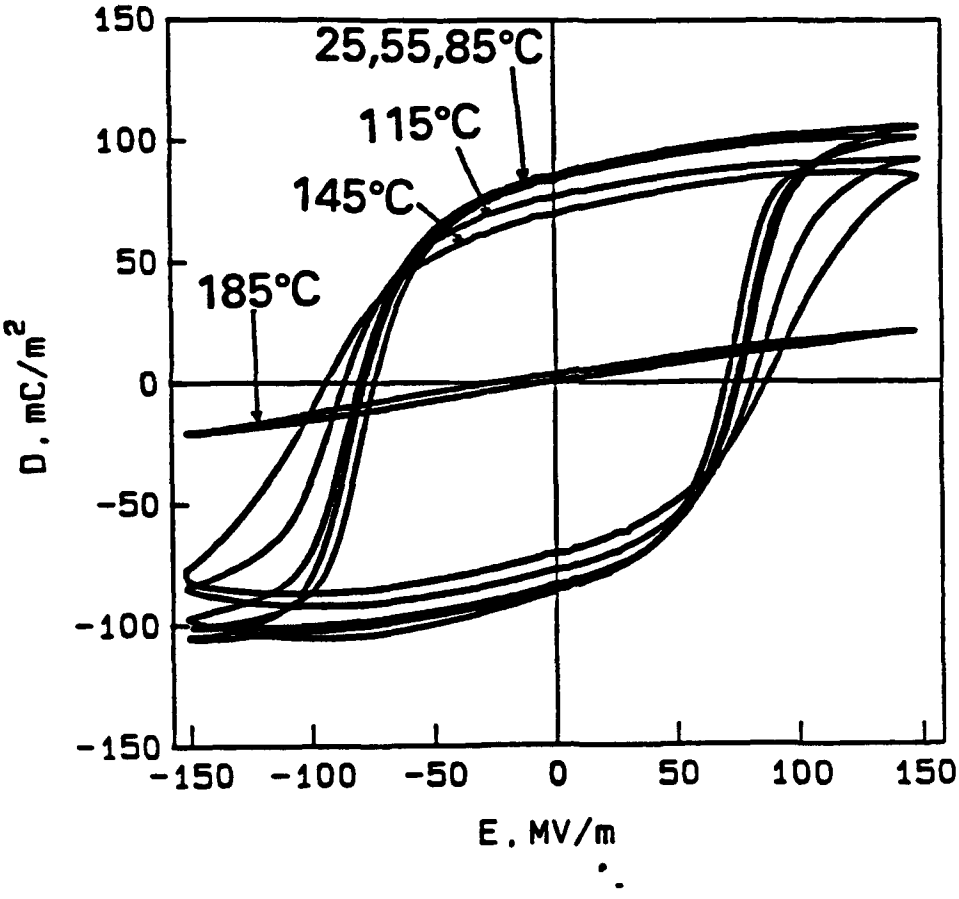
25,55,85°C
115°C
145°C
185°C
150
100
50
0
-50
-100
-150
-150 -100 -50 0 50 100 150
D, mC/m²
E, MV/m

Fig. 4

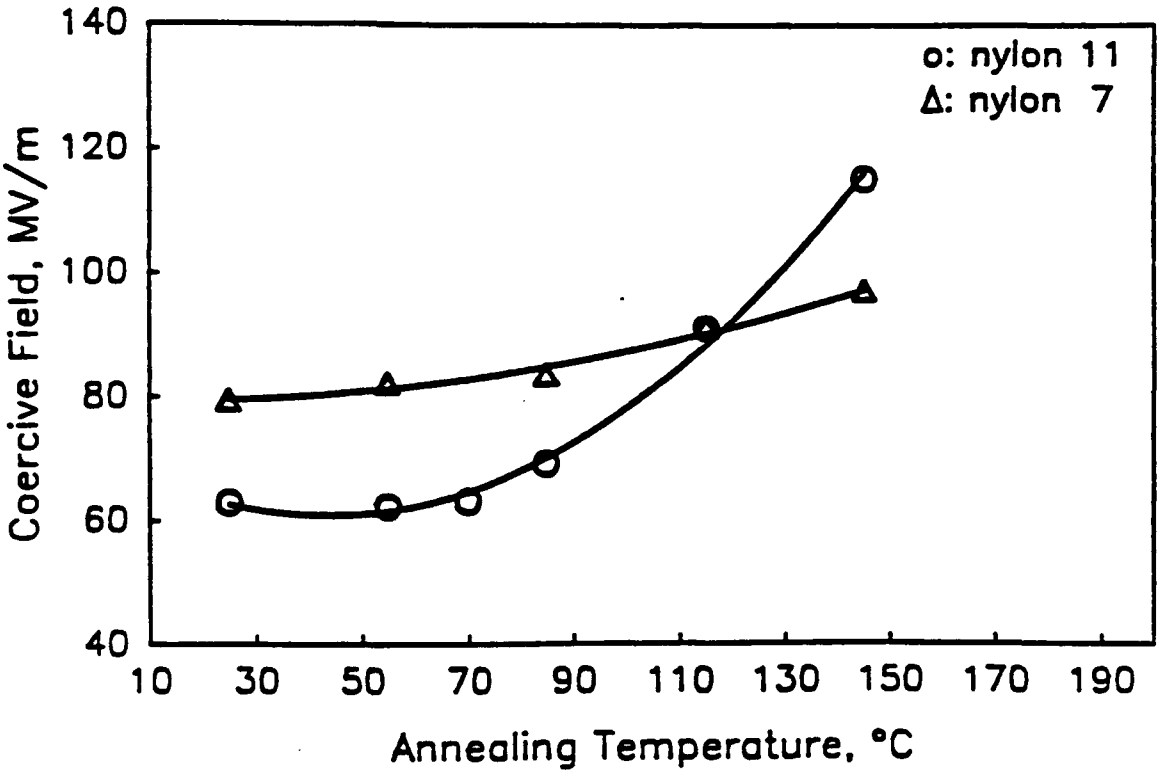
140
120
100
80
60
40
Coercive Field, MV/m
o: nylon 11
Δ: nylon 7
10
30
50
70
90
110
130
150
170
190
Annealing Temperature, °C

Fig. 5

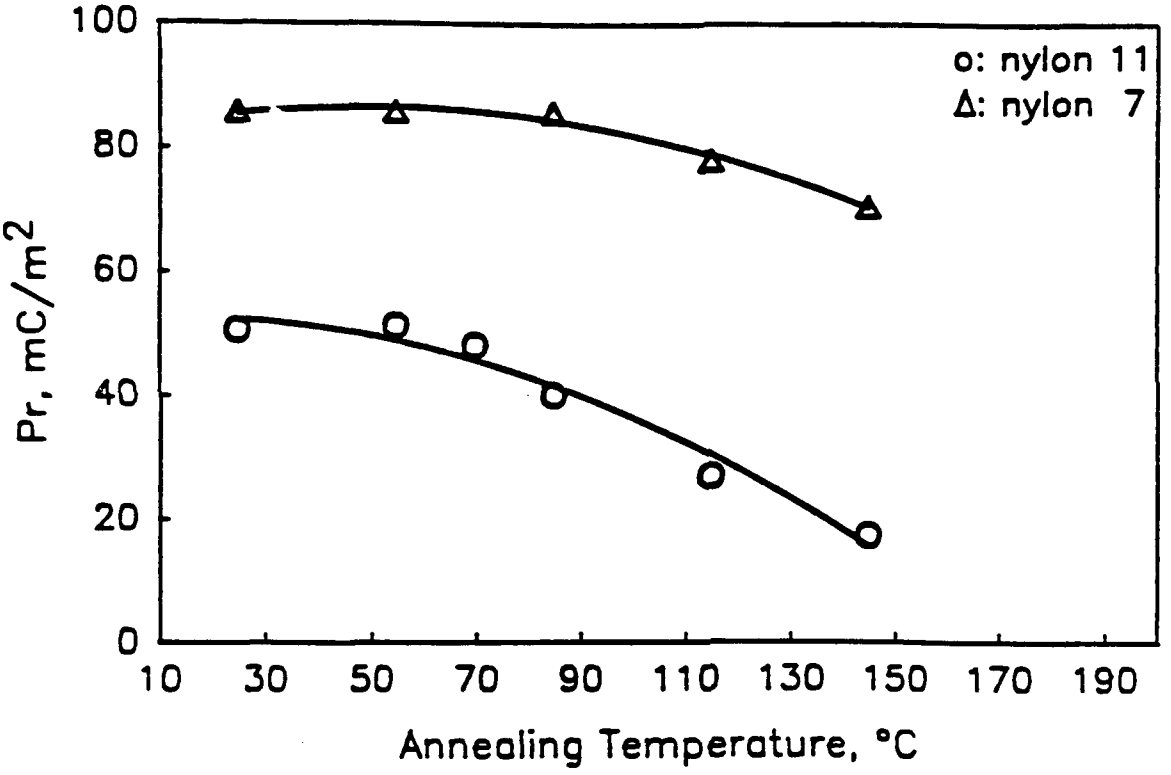
100
80
60
40
20
0
Pr, mC/m2
o: nylon 11
Δ: nylon 7
10
30
50
70
90
110
130
150
170
190
Annealing Temperature, °C

Fig. 6

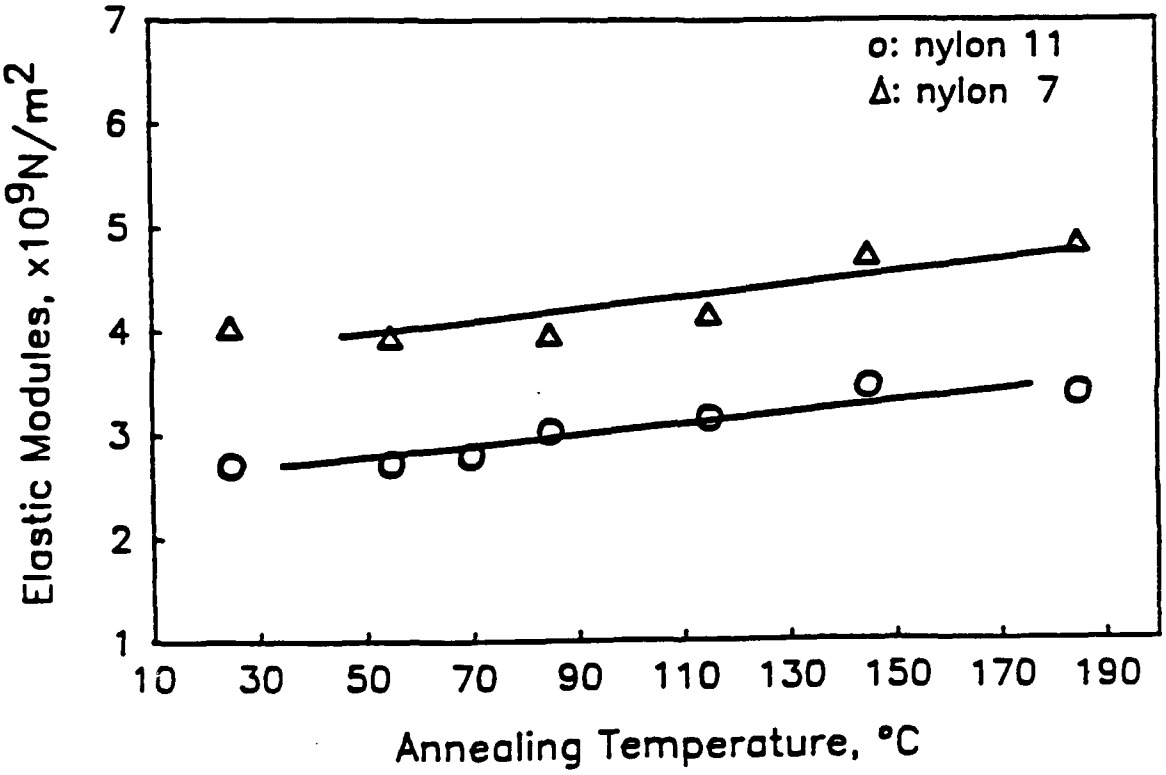
o: nylon 11
Δ: nylon 7
Elastic Modules, x10^9N/m^2
Annealing Temperature, °C
1
2
3
4
5
6
7
10
30
50
70
90
110
130
150
170
190

Fig. 7

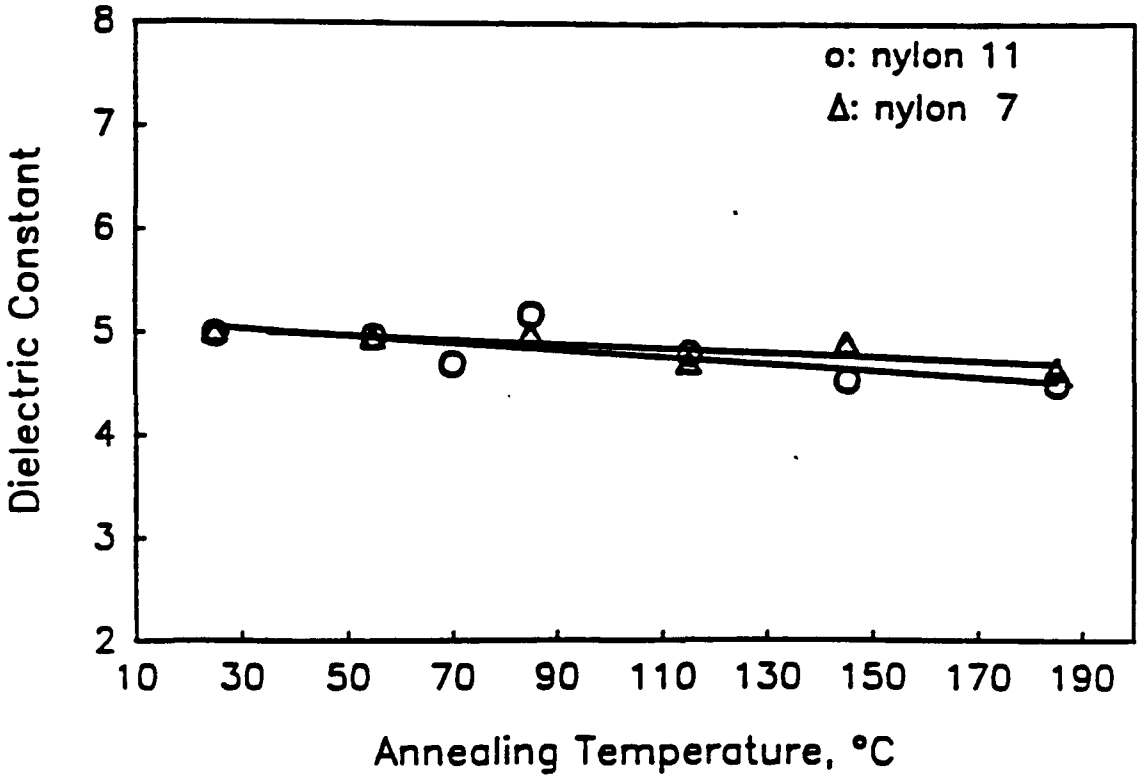
o: nylon 11
Δ: nylon 7
Dielectric Constant
8
7
6
5
4
3
2
10
30
50
70
90
110
130
150
170
190
Annealing Temperature, °C

Fig. 8

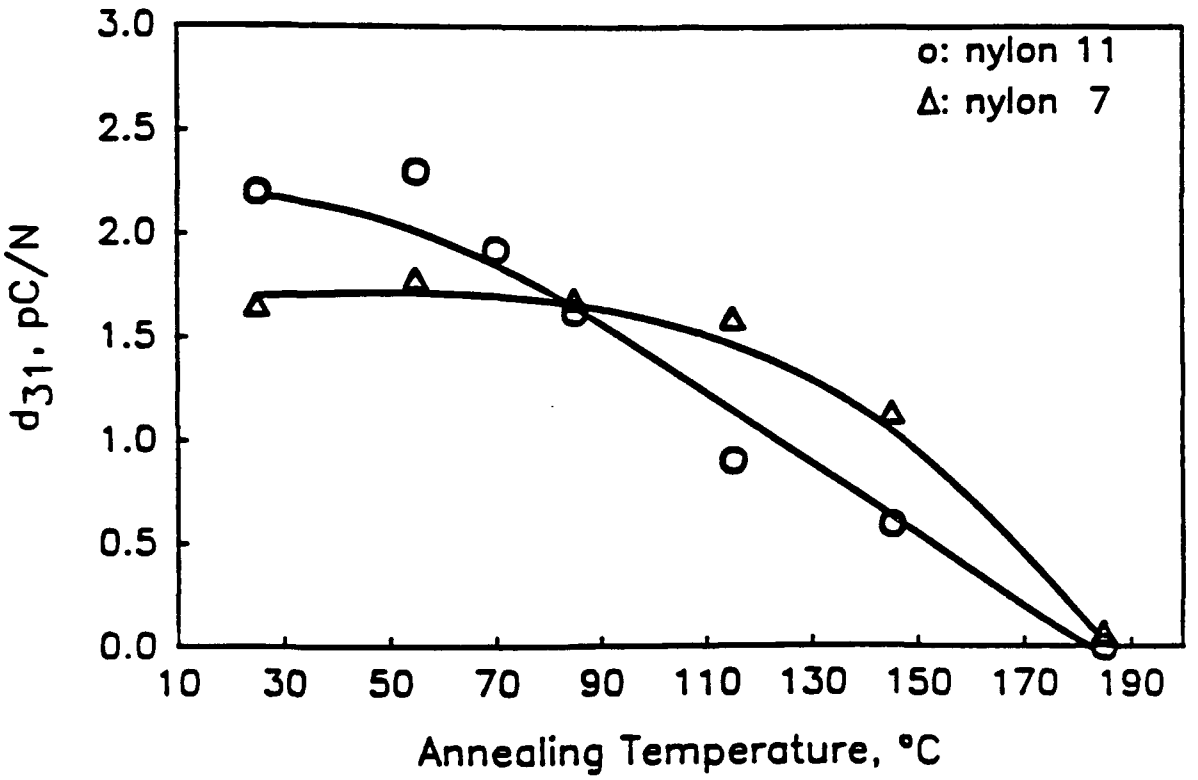
3.0
2.5
2.0
1.5
1.0
0.5
0.0
d_{31}, pC/N
o: nylon 11
Δ: nylon 7
10
30
50
70
90
110
130
150
170
190
Annealing Temperature, °C

Fig. 9

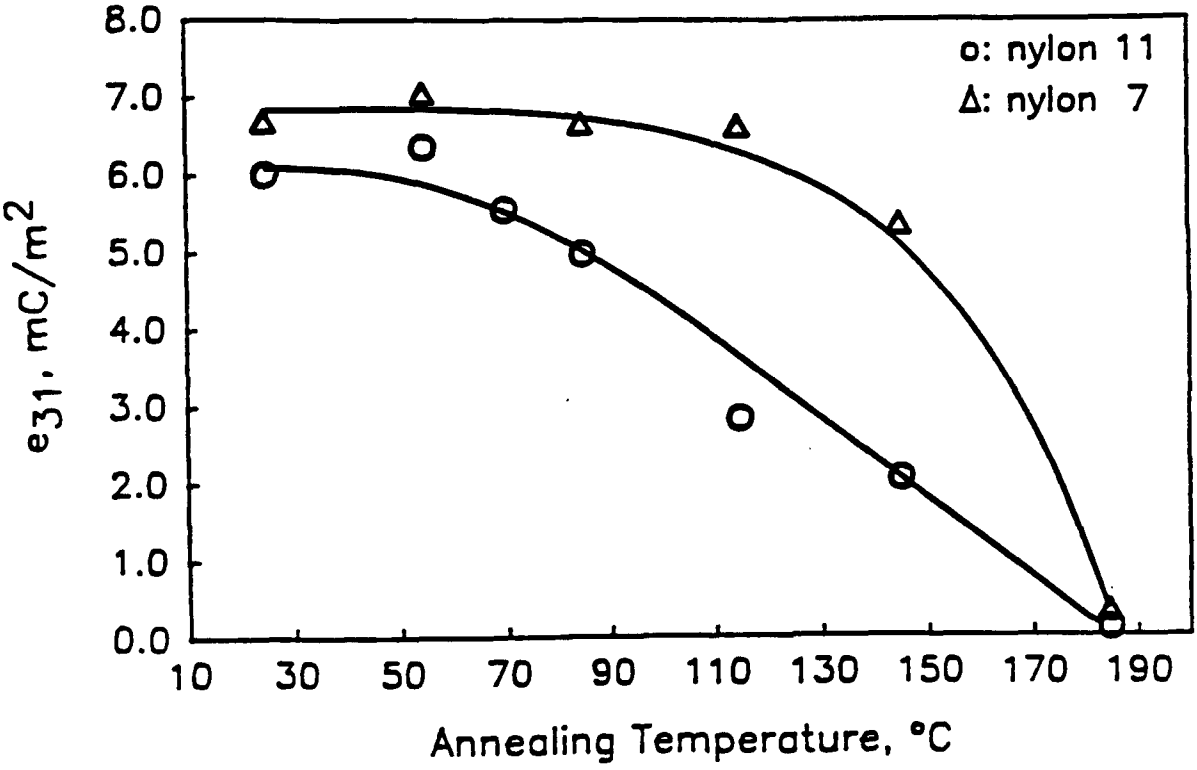
8.0
7.0
6.0
5.0
4.0
3.0
2.0
1.0
0.0
e_{31}, mC/m^2
o: nylon 11
Δ: nylon 7
10
30
50
70
90
110
130
150
170
190
Annealing Temperature, °C

Fig. 10

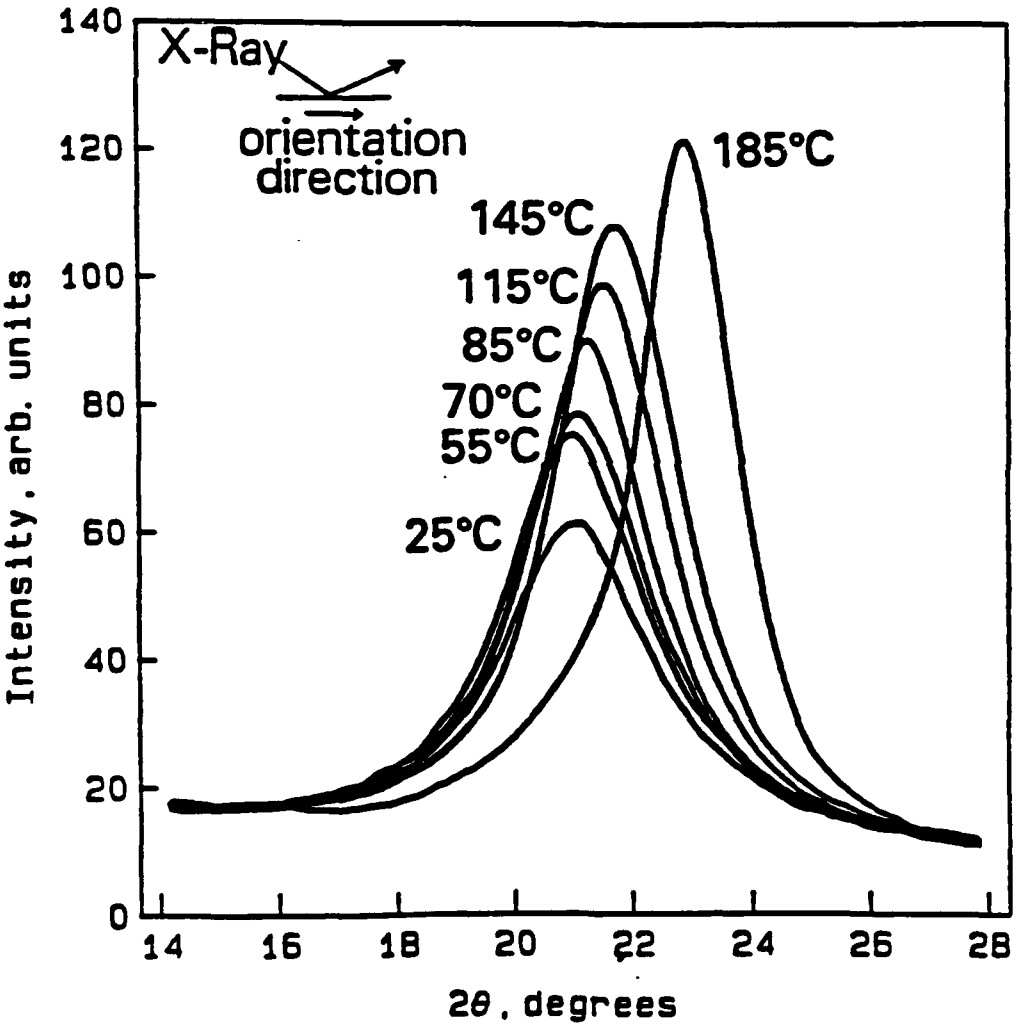
X-Ray
orientation direction
185°C
145°C
115°C
85°C
70°C
55°C
25°C
Intensity, arb. units
2θ, degrees
0
20
40
60
80
100
120
140
14
16
18
20
22
24
26
28

Fig. 11

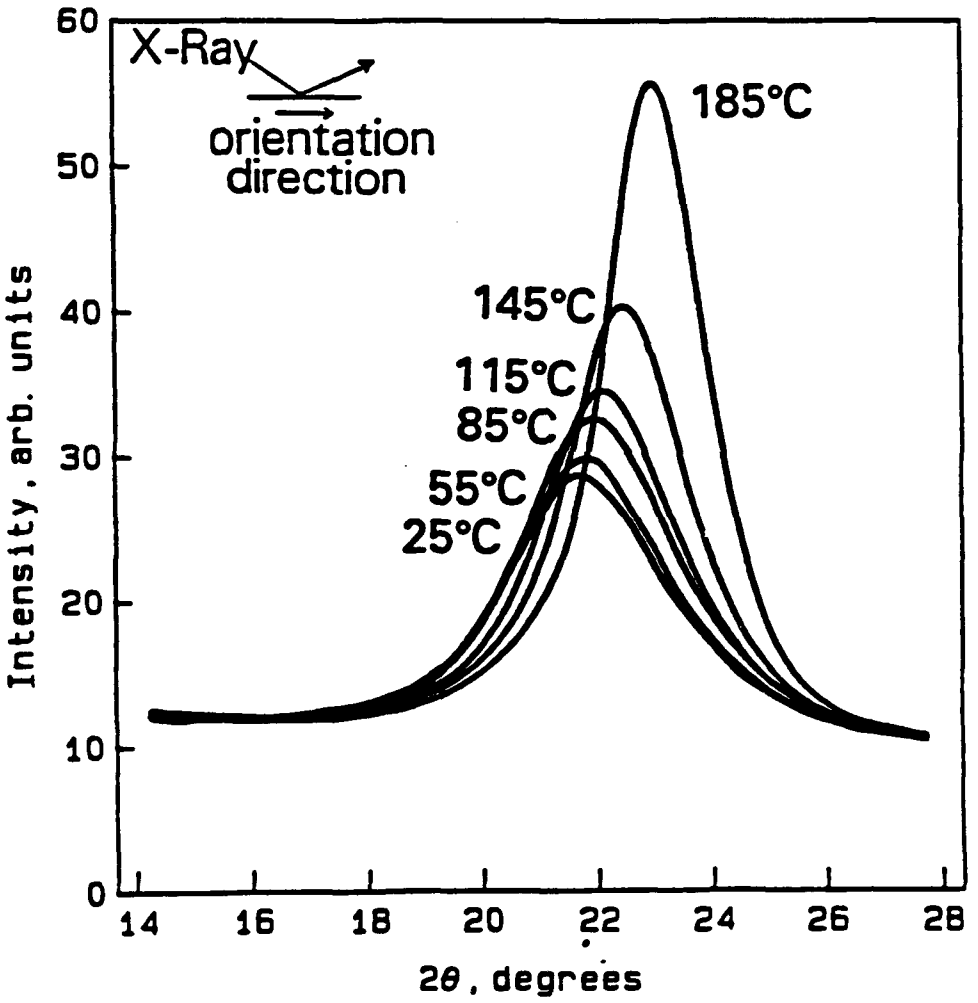
X-Ray
orientation direction
185°C
145°C
115°C
85°C
55°C
25°C
Intensity, arb. units
2θ, degrees
0
10
20
30
40
50
60
14
16
18
20
22
24
26
28

Fig. 12

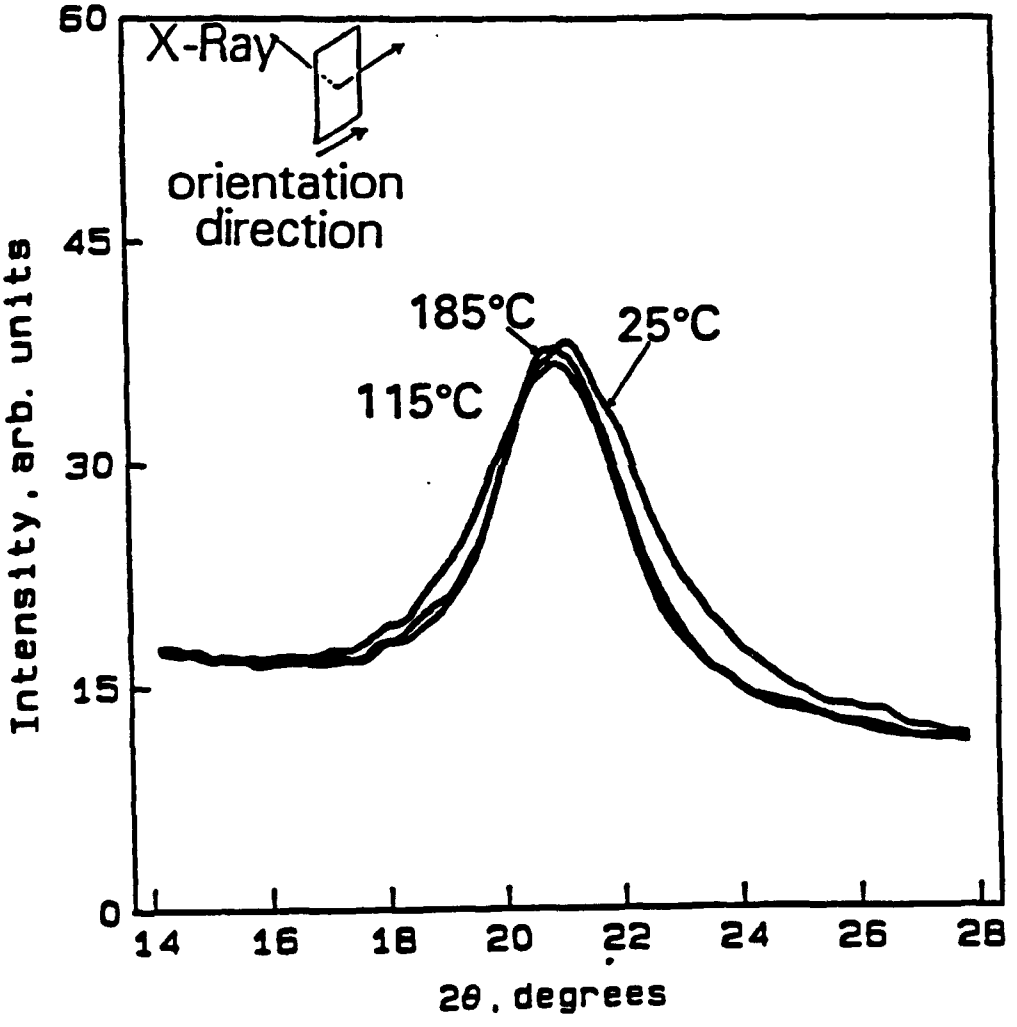
X-Ray
orientation direction
185°C
25°C
115°C
Intensity, arb. units
60
45
30
15
0
14
16
18
20
22
24
26
28
2θ, degrees

Fig. 13

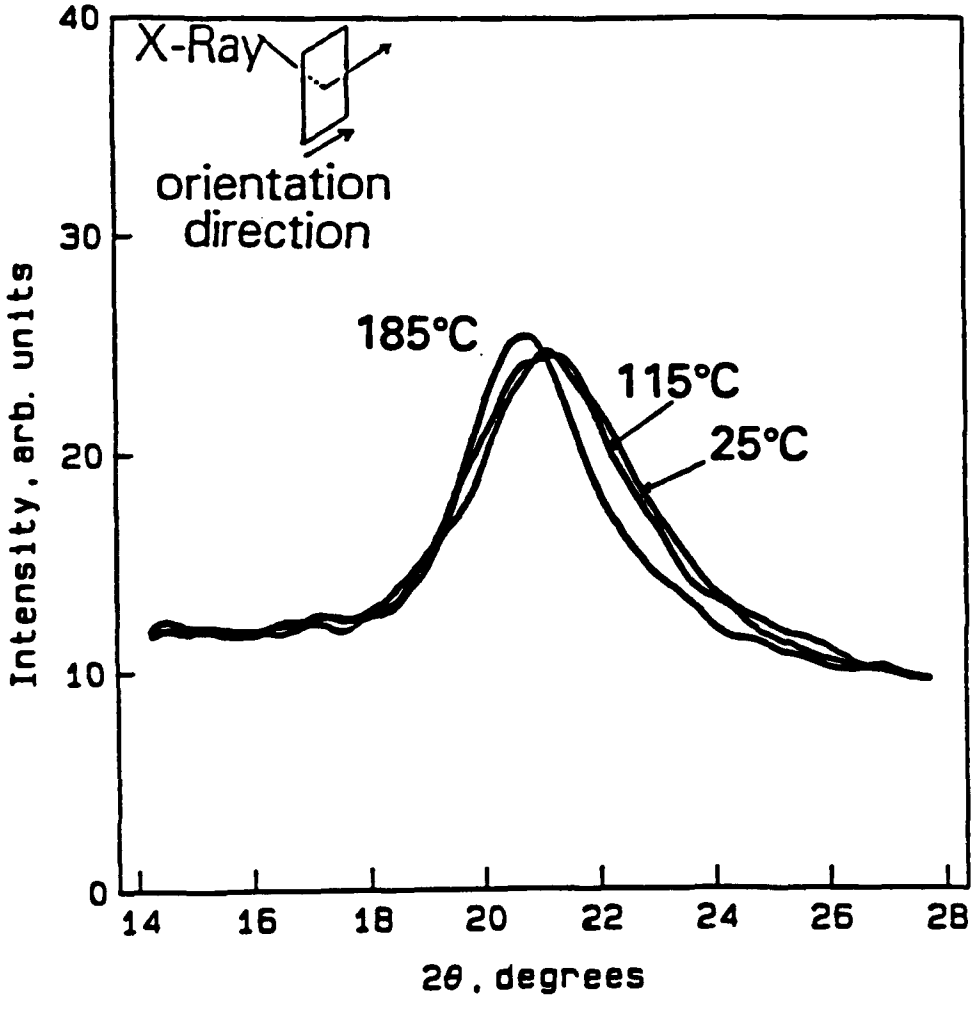
X-Ray
orientation direction
185°C
115°C
25°C
Intensity, arb. units
0
10
20
30
40
14
16
18
20
22
24
26
28
2θ, degrees

Fig. 14

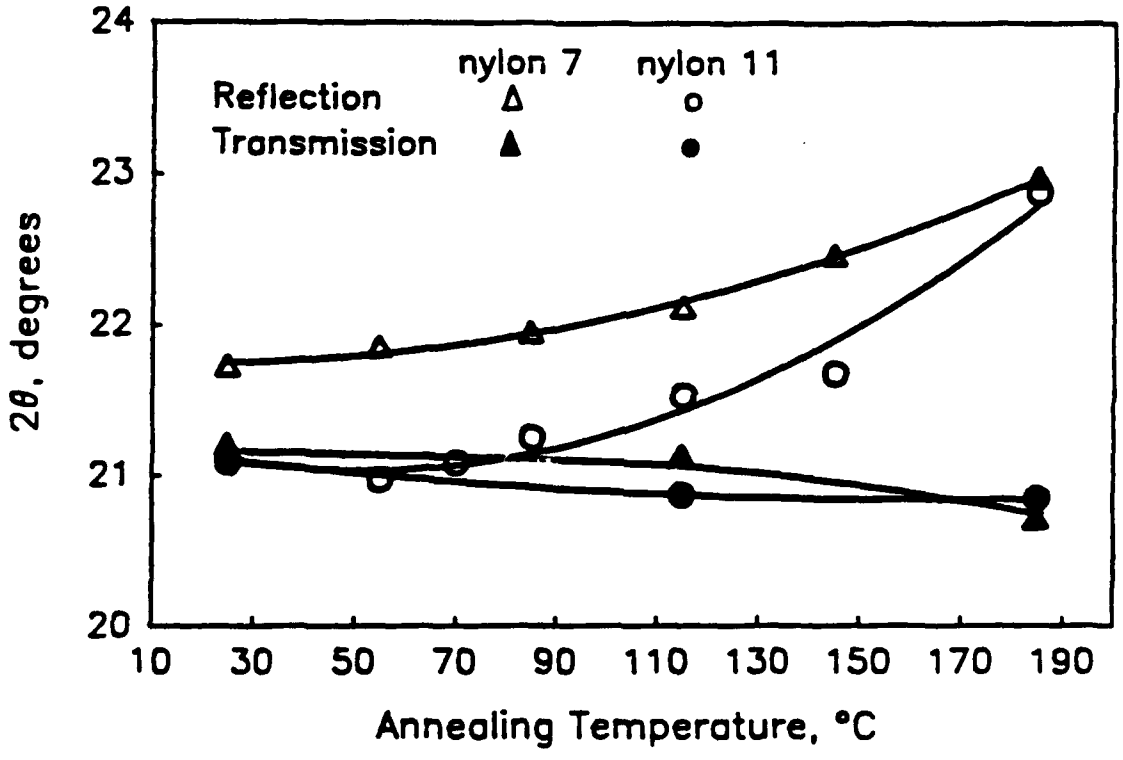
24
23
22
21
20
2θ, degrees
nylon 7
nylon 11
Reflection
Transmission
10
30
50
70
90
110
130
150
170
190
Annealing Temperature, °C

Fig. 15

Effect of TCP Doping on the Remanent Polarization in Uniaxially Oriented Poly(Vinylidene Fluoride) Films

Y. Takase,* J. I. Scheinbeim, and B. A. Newman

Department of Mechanics and Materials Science, College of Engineering, Rutgers University, Piscataway, New Jersey 08854

ABSTRACT: Uniaxially stretched films of poly(vinylidene fluoride) were doped (1 wt. %) with plasticizer, tricrecyl phosphate (TCP). This slight doping with TCP was found to enhance the amount of remanent polarization in the region of low poling fields (e. g. from 1 to 6 mC/m^2 under E_p = 60 MV/m at 20°C) and high poling fields (e. g. from 57 to 66 mC/m^2 under E_p = 200 MV/m at 20°C). The pyroelectric coefficient has shown that the doping enhances a quite stable (up to about 140°C) remanent polarization after high field poling (e. g. from 10.2 to 12.5 $\mu C/m^2/K$ under E_p = 200 MV/m at 20°C). This is suggestive of a field induced increase in crystallinity. In addition, the switching of quasi-stable dipoles (those which randomize in the 90 - 140°C range) takes place at much lower electric fields than in undoped films. The present data suggest that a small amount of dopant in the noncrystalline regions greatly enhances ferroelectric dipole switching, possibly by acting in the interfacial zone between crystalline and amorphous regions.

Introduction

Plasticized polymers, such as the poly(vinyl chloride)-tricrecyl phosphate (PVC-TCP) system, offer significant advantages in their physical properties such as toughness, flexibility, oil-resistance, and non-flammability as well as high electrical resistance when compared to unplasticized polymers.

Recently, it was found in our laboratories that the addition of plasticizer to poly(vinylidene fluoride) (PVF_2) films has a significant influence on their piezoelectric and pyroelectric properties. Sen et al.[1] prepared two different types of samples to examine the effects of TCP doping. One type of sample was unoriented phase II PVF_2 film which was prepared by melt crystallization. The other type of sample was oriented phase I PVF_2 film which was obtained from the phase II film by uniaxial stretching at 54°C. For doping, the film was immersed in TCP at elevated temperatures.

In the case of the initially unoriented phase II films, the piezoelectric and pyroelectric coefficients of the doped films showed significantly improved values compared to those of the undoped films when poled under identical conditions. The results of X-ray diffraction studies of both types of samples showed that for the doped films, the phase transformation from the nonpolar phase II crystal form to the polar phase I crystal form had taken place at much lower poling fields than for undoped films.

In the case of the uniaxially oriented phase I films, doping also led to a large increase in piezoelectric and pyroelectric response.

Although X-ray diffraction data of the doped films have suggested that some preferential positioning of the dopant at the crystallite boundaries may occur, with no evidence of diffusion of the dopant into the crystalline regions, additional studies are required to gain some understanding of the mechanisms involved.

PVF_2 is a semicrystalline polymer and its crystallinity is usually around 50 %[2-5] (recently, perdeuteriated PVF_2 films were found to have much higher crystallinity[6]). Since there was no indication (from X-ray diffraction studies) of the plasticizer diffusing into the crystalline regions,[1] most of the plasticizer must be in solution outside the crystalline regions. The effect of the plasticizer on the bulk properties of PVF_2 film may therefore be understood in terms of the activity of the dopant on a heterogeneous system which consists of crystalline regions and plasticized amorphous regions and their interface zones.

One possible way to identify the role of plasticizer in this complicated system is to only slightly dope the sample to ensure that the plasticizer does not change too many physical parameters simultaneously (i. e. modulus, dielectric constant, thermal expansion) and to detect any significant effects by some set of sensitive measurements. Our assumption of the minimal effects of the slight doping (about 1 wt. % as described later) with plasticizer on the physical properties of the films is based on the fact that a polymer which is ~ 70°C above its glass transition temperature (~ -50°C for PVF_2) will exhibit minimal changes in properties at room temperature.

A recent study carried out by Takase et al.[7] on the

polarization reversal characteristics of PVF_2 provides suggestions concerning such measurements. They used a γ-ray irradiation technique in order to identify the different roles of dipoles whose arrangement covers a range from an amorphous state to a well ordered crystalline state. This study was based on the assumption that molecular chains within the crystals are less affected by γ-ray irradiation than chains in the amorphous regions.[8] It was found that the effect of irradiation was most pronounced during the initial stage of the polarization reversal process i. e. on the nucleation stage.[7] A very likely place for the nucleation process to occur is the interfacial zone between the crystalline and amorphous regions. If we add a small amount of dopant to the PVF_2 film, we should observe an effect which may be a counterpart to the γ-ray irradiation effect, i. e. something which appears not to alter the crystalline regions while slightly altering the amorphous regions and the interface zones.

In the present study, we prepared doped samples by the same immersion method used by Sen et al.[1] but we changed some sample and measurement conditions. We used the same stretched films previously used by several other researchers for polarization reversal measurements,[7,9-12] to examine consistency with previous data. We limited the temperature and time of the immersion process to much less than those used by Sen et al.,[1] so as to minimize change in the physical condition of the crystalline regions and we then examined the change in remanent polarization, P_r, which is the most fundamental parameter related to piezoelectric and pyroelectric properties.

As a result, we hoped to show some marked effect of the dopant on the electric displacement, D, on the depolarization current (DPC) and on the pyroelectric coefficient, p_y, of the PVF_2 films. Based on detailed data obtained under various poling conditions, the role of the dopant in enhancing the remanent polarization was examined.

Experimental Section

Samples used in this study were 7-μm-thick uniaxially oriented PVF_2 films (KF1000) supplied by Kureha Chemical Industry, Co., Ltd. These films are the same as those used in several previous studies[7,9-12] and, in addition, 97 % of the crystalline material is in the phase I form.[10] Annealed samples were prepared by heat treatment in vacuum at 120°C for 2 hours. During annealing, the film was mechanically clamped to prevent shrinkage.

Doped samples were prepared by immersing the annealed films in tricresyl phosphate at 100°C for 4 hours. The temperature and immersion time were much less than those used (130°C for 24 hours) by Sen et al.[1] The dopant content was only about 1 % by weight. Hereafter, undoped sample refers to the as annealed undoped film.

Gold electrodes, each about 3 x 10 mm^2 in area, were deposited on opposing surfaces of the films by vacuum evaporation. All measurements, except X-ray measurements, were carried out by placing the sample in an electrically shielded copper cell which was equipped with a heater and temperature

sensor.

X-ray diffraction profiles were obtained at room temperature with a Philips XRG 3100 X-ray generator. CuK_{α} radiation filtered with a Ni foil was used.

The D - E hysteresis characteristics were measured at 20°C using a high voltage power supply and a picoammeter (Keithley 485) connected in series with the sample. The period of the triangular shaped high voltage wave was 1000 s.

The pyroelectric coefficient and depolarization current were obtained from samples poled by applying a step voltage pulse of 1 min width at room temperature; then, the thermally stimulated current was measured by the picoammeter as the sample was subjected to heating and cooling cycles at a rate of 2°C/min.

Operation of various functions in the system were consigned to a microcomputer (IBM-XT) which also performed the task of data processing.

Results

1. X-ray Diffraction Profiles. The diffractometer scans for the five samples, as-received, annealed, annealed-doped, annealed-poled and annealed-doped-poled, in the reflection mode are shown in Figure 1 (a). Figure 1 (b) shows the current densities, J, obtained during the poling procedure at room temperature for the doped and undoped samples. For the X-ray measurements, all samples were prepared and chosen so that there were no significant differences in sample dimensions (unmetalized fringe areas and the Gold electrodes were removed). Table I shows the

2θ values and half widths, $\beta_{1/2}$, for the composite (110)(200) reflection of the phase I crystals in the above five samples. It is seen that the annealed sample exhibits a larger 2θ value, a smaller half width and a larger peak height than the as-received samples, indicating a decrease in interplaner separation caused by better packing and increased perfection and size of the crystallites. This is the major change found in the diffraction profiles among the five samples.

The doped sample does not exhibit significant change in 2θ value and half width from those of the annealed sample, although there is probably a slight additional annealing effect caused by the immersion in TCP at 100°C for 4 hours. Actually, the annealed sample, which was heat treated by additional annealing at 100°C for 4 hours, also exhibited similar slight change in 2θ value. The doping process did not cause the phase I crystalline material to transform to other phases. The doping did not broaden the half width. Therefore, as expected, the low level of dopant did not appear to diffuse into or significantly affect the structure of the crystalline regions.

The poled samples, both doped and undoped, exhibit large secondary changes in their diffraction profiles; a larger 2θ value, a smaller half width and a larger peak height than the unpoled samples. This is indicative of a certain amount of crystal growth as well as the better chain packing induced by the electric field . After testing several samples, the doped and poled samples had a tendency to exhibit the largest changes in their X-ray diffraction profiles; a typical result is shown in Figure 1 (a). The remanent polarization, P_r, obtained by inte-

grating J with respect to time is 69 and 60 mC/m^2 for the doped and undoped samples, respectively (showing slightly larger values than those obtained in the next section because there was no correction for the dc conduction current). The doped sample exhibits a 15 % higher P_r value than the undoped sample. The increase in P_r is consistent with the X-ray diffraction data indicating a certain amount of crystal growth.

2. D - E Hysteresis Characteristics. Figures 2 (a) and (b) show current density, J, and electric displacement, D, respectively, as a function of electric field, E, when the samples are subjected to triangular electric field pulses with maximum fields of 60, 120 and 200 MV/m. The dotted lines represent data for the doped samples and the continuous lines for the undoped samples. In this measurement, the doped sample showed a certain amount of dc conduction. The conduction component consists of an ohmic (linear) component and a nonlinear component. The nonlinear component normally obeys an exponential dependence on the electric field. Figure 2 (a) shows the corrected J vs E characteristics obtained by subtracting the conduction components.

Fig.2(a)
Fig.2(b)

Significant differences are observed between the data of the doped and undoped samples. The doped samples show a well defined peak on the J - E curves (Figure 2 (a)), even if the peak value of E, E_p, is comparatively low; around 60 MV/m. The D - E hysteresis curve (Figure 2 (b)), corresponding to the J - E curve for E_p = 60 MV/m, exhibits a certain amount of remanent polarization (11 mC/m^2). On the other hand, the undoped sample does not show the peak and exhibits a propeller like D - E hysteresis curve

(Figure 2 (b)), which indicates that a small number of dipoles orient under the application of an electric field of 60 MV/m but their orientation is not stable enough to exhibit remanent polarization. These data indicate that ferroelectric dipole orientation is significantly enhanced by the presence of a small amount of TCP outside the crystalline regions of the film.

When the amplitude of the field is 120 MV/m, the doped sample shows a sharp peak on the J - E curve (Figure 2 (a)). Under this field, the undoped sample shows a broad peak on the J - E curve, indicating a polarization reversal originating from some initial field induced (crystal) dipole orientation. Both samples exhibit almost the same amount of remanent polarization, as is indicated on the D - E hysteresis curves (Figure 2 (b)).

When the field amplitude becomes as high as 200 MV/m, each sample shows a sharp peak on the J - E curve (Figure 2 (a)). The value of remanent polarization of the undoped sample, about 57 mC/m^2 as indicated on the D - E curve (Figure 2 (b)), is known to be almost a saturated value at 20°C.[11] The doped sample, however, exhibits a value of about 66 mC/m^2 (average value of $+P_r$ and $-P_r$ in Figure 2 (b)) which is 16 % larger than that of the undoped sample and is consistent with the data in Figure 1 (b). The J - E curve (Figure 2 (a)) indicates that the increase in P_r of the doped sample is caused by an increase in the current component of polarization reversal in the field region higher than the coercive field. It is surprising that only 1 wt. % of dopant enhances the remanent polarization by 16 % in the high poling field region as well as the large enhancement of P_r in the low poling field

region.

3. Depolarization Current. The D - E hysteresis characteristics show the essential features of ferroelectric polarization reversal and give the value of remanent polarization; however, they do not reveal sufficient information about the polarization reversal mechanism, especially of semicrystalline polymers. In such polymers, not only does the dipole motion within the crystallites differ from that outside but also differs among crystallites; several physical parameters depend on crystallite size.[13-15] The depolarization current of ferroelectric materials yields information about the thermal stability of the oriented dipoles which reflects their environment in the amorphous regions, the microdomains in small crystallites, and domains in the "usual" crystallites.

The depolarization current densities of the doped and undoped samples are shown in Figures 3 (a) and (b), respectively. Curves (1) - (4) represent the current density for samples poled by a 1 min step pulse of 20, 60, 120, and 200 MV/m field strength, respectively, and curve (5) poled by sequential step pulses of 200 MV/m strength applied in opposite directions. Both samples exhibit one or two current density peaks over the temperature measurement region. A low temperature peak appears in the temperature region 30 - 40°C and the peak shifts slightly to the high temperature side as the poling field increases. A high temperature peak appears around 90°C when the poling field is 20 and 60 MV/m. This peak shifts rapidly to the high temperature side as the poling field increases.

Fig. 3(a)
Fig. 3(b)

The marked effect of dopant is also present in the depolarization current. When the poling field is comparatively low, the doped sample shows much higher first and second peaks than those of the undoped sample. The increase in the second peak is prominent after doping; the height is five times larger than that of the undoped sample at E_p = 60 MV/m (see curve (2)). When the field is as high as 200 MV/m, the second peak shifts to a temperature region higher than 140°C and only the broad tail of it can be seen for the doped sample (see curve (4)). After applying a second poling field in the reverse direction, the first peak height (of curve (5)) increases to twice the size of that (of curve (4)) of the sample poled using a single step pulse and the height difference of the first peak between the two types of samples is reversed (see curve (5) in Figures 3 (a) and (b)).

Figure 4 presents the depolarization current vs temperature data which look at the effects of the polarization reversal process for both the doped (dotted lines) and the undoped (continuous lines) samples. Curve (1) represents characteristics of the sample poled under E_p = +200 MV/m, and curve (2) for the sample poled under E_p = +200 MV/m and then E_p = -200 MV/m. These two curves are essentially symmetric with respect to the temperature-axis, indicating complete polarization reversal.

Figure 4

Curves (3) and (4) represent characteristics of the samples which are subjected to the poling sequence +200 MV/m, -200 MV/m, followed by polarization reversal produced by applying field of E_p = +20 and +40 MV/m, respectively. This was done to gain some further insight into the polarization reversal process. This will be discussed later.

4. Pyroelectric Coefficient. PVF_2 does not show a ferroelectric to paraelectric phase transition before melting occurs; therefore, it is impossible to know the total remanent polarization of the sample by simple integration of the depolarization current (DPC) unless the sample is taken to the melting point. However, we can estimate P_r from the pyroelectric coefficient, p_y, since it is proportional to the remanent polarization.[16]

Figures 5 (a) and (b) show the p_y vs T characteristics of the doped and the undoped samples, respectively. The value of p_y is calculated from the DPC on the cooling cycle after heating up to 140°C, so that p_y reflects only the high temperature stable remanent polarization. p_y is obtained from the relation:

Fig. 5(a)
Fig. 5(b)

$$p_{yi} = (J_i - J_{i-1})(t_i - t_{i-1})/(T_i - T_{i-1}), \quad (1)$$

where J is the current density, t the time, T the temperature and the subscript i denotes the sampling number. Curves (1) - (9) represent data obtained under different poling conditions as follows; (1) - (5): a step pulse of +20, +80, +120, +160, and +200 MV/m, respectively, (6): sequential step pulses of +200, -200 and +200 MV/m, (7): a step pulse of +200 MV/m followed by -200 MV/m, (8): sequential step pulses of +200, -200 and +20 MV/m, and (9): sequential step pulses of +200, -200 and +40 MV/m.

When the poling field is 80 MV/m or lower, the value of p_y is essentially zero indicating complete decay of the remanent polarization after the process of heating up to 140°C. Therefore, integration of the depolarization current up to 140°C gives the

remanent polarization; for example the integration of curve (2) in Figure 3 gives 6 mC/m^2 and 1 mC/m^2 under E_p = 60 MV/m for doped and undoped samples, respectively. These values are essentially consistent with the hysteresis data (P_r = 11 and 1 mC/m^2 shown in Figure 2 (b)) since the DPC is measured sometime after poling and some of the unstable polarization has decayed. As the poling field increases up to 120 MV/m, the value of p_y slightly increases for both doped and undoped samples. This is consistent with the DPC data, since the tail of the second peak goes into the temperature region above 140°C (see Figure 3). The increase in poling field from 120 to 160 MV/m brings about a large increase in p_y, from -0.9 to -5.7 $\mu C/m^2/K$ at 40°C, for the doped sample and -0.9 to -4.5 $\mu C/m^2/K$ at 40°C for the as-annealed sample. This is indicative of a large enhancement of the stable remanent polarization which does not decay by heating up to 140°C. It is also clear that the stable remanent polarization increases when the sample is poled by a train of electric field step pulses applied in reversed directions. When the sample is poled in a reversed direction, the polarity of p_y reverses. The value of p_y of the doped samples after the reversal is 12.5 $\mu C/m^2/K$, which is larger by 22 % than the 10.2 $\mu C/m^2/K$ of the as-annealed samples. This is also quite consistent with the D - E hysteresis data (16 % increase in P_r as shown in Figure 2(b)).

Discussion

1. Dopant Effect in the Low Poling Field Region. When the samples are poled below about 80 MV/m, the dopant effect is the

most prominent. The amount of P_r in the doped sample is several times larger than that of the undoped samples under identical poling conditions. The DPC measurements indicate that P_r originates from the orientation of thermally unstable dipoles which totally randomize on heating up to 140°C. The fact that this effect is strongest at low poling fields may indicate that the thermally unstable dipoles are located in an environment which is directly affected by the noncrystalline regions where the dopant exists.

2. Dopant Effect in the High Poling Field Region. A marked dopant effect is observed after polarization reversal; the 15 - 16 % increase in the remanent polarization and the 22 % increase in the pyroelectric constant after repeated application of high reversed poling fields. A possible mechanism involved is additional crystal growth at the interfacial zones, which is indicated by the X-ray diffraction data shown in Figure 1 (a) and is consistent with previous studies.[17,1] An additional increase in the internal field in the crystalline regions due to an increase in dielectric constant in the amorphous regions, and an increase in thermal expansivity may be other mechanisms. In the present experiments, however, the doped samples showed about a 16 % increase in P_r which was almost independent of the dc conduction levels of the samples tested (see Figure 1 (b) and Figure 2 (b)), and the measurements of dielectric constant and mechanical modulus showed no significant measurable change after the doping. The fact that a small amount of dopant produced a large change in the P_r and p_y values suggests to us some catalytic role of the

dopant rather than a more macroscopic role related to changes in bulk dielectric constant or mechanical properties.

3. Dopant Effect on the Polarization Reversal Process. In order to further understand the dopant effect, it is useful to examine the two sets of data of DPC vs T (Figure 4) and p_y vs T (Figure 5) since they reveal some details of the process of polarization reversal. Figure 6 shows the behavior of DPC and p_y at a fixed temperature after application of a reversal poling field. Curve (1) is the trace of p_y at 40°C, a part of which is shown in Figure 5 (b). Since p_y is obtained in the cooling cycle after heating up to 140°C, the curve represents the polarization reversal process of the thermally stable dipoles. Curves (2) and (3) are the traces of the depolarization current densities (in Figure 4) at 135°C for doped and undoped samples, respectively. Since the current is measured in a heating cycle, the curves represent the polarization reversal process of the thermally unstable dipoles. The thermally stable dipoles do not reorient if the antiparallel field is lower than about 80 MV/m and suddenly begin to switch around E_p = 100 MV/m (see curve (1) in Figure 6). This behavior appears to indicate switching of dipoles in the crystalline regions. On the other hand, the thermally unstable dipoles tend to reorient, even if the antiparallel field is lower than 20 MV/m (curves (2) and (3)). This behavior suggests that the switching of the thermally unstable or quasi-stable dipoles occurs in the noncrystalline or interface regions. If we define an apparent coercive field, E_c as the intercept of curves (1), (2) and (3) or the E_p axis, they are about 100, 25 and 55 MV/m,

Figure 6

respectively. The large decrease in E_c from 55 to 25 MV/m is one of the most prominent dopant effects in the polarization reversal process. We can see an intimate relation between the decrease in E_c and the data of the hysteresis measurement. The J vs E curves in Figure 2 (a) show that the peak position of the doped sample under E_p = 60 MV/m is about 40 MV/m, while the undoped sample does not show the peak. The peak position of the undoped sample, however, was estimated to be around 90 MV/m from the additional measurement under E_p = 100 MV/m. The peak position under low E_p also represents a coercive field of the quasi-stable dipoles. Therefore, it is considered that more than half of the decrease in coercive field which appeared in both D - E and DPC measurements reflected a prominent doping effect of the quasi-stable dipoles.

It is interesting to note that the behavior of dipoles with different stability in PVF_2 is also clear in the time domain measurement of the polarization reversal.[7] The dopant effect shown by the large decrease in E_c for the unstable dipoles is also quite consistent with the effect of γ-ray irradiation[7] on the polarization switching characteristics. Irradiation suppresses the nucleation probability while the presence of dopant appears to produce exactly the opposite effect. The dopant effect as well as the γ-ray irradiation effect on the polarization reversal process may provide further information about the nucleation and domain growth process in PVF_2 films.

Conclusions

X-ray diffraction data show that the dopant exists outside the crystalline regions of the film; however, even this small amount of TCP (1 wt. %) significantly enhances the low poling field (E_p < 80 MV/m at room temperature) remanent polarization. The polarization originates from thermally unstable dipole orientation, which is suggestive of their environment: interfacial zones between crystalline and amorphous regions. Doping with TCP also enhances the high poling field (E_p > 120 MV/m at room temperature) remanent polarization. The polarization originates from a thermally stable dipole orientation, which is suggestive of a certain amount of crystal growth at the interfacial zones.

In the polarization reversal process, doping with TCP greatly decreases the coercive field of dipoles which might exist at the nucleation sites of polarization domains, i. e. at the interfacial zones. This may provide further information about the nucleation and growth process during polarization reversal in PVF_2 films.

Acknowledgment. This work was supported by DARPA and the Office of Naval Research.

References and Notes

(1) Sen, A.; Scheinbeim, J. I.; Newman, B. A. J. Appl. Phys. 1984, 56, 2433.

(2) Kakutani, H. J. Polym. Sci. 1970, 8, 1177.

(3) Murayama, N. J. Polym. Sci. 1975, 13, 929.

(4) Kepler, R. G.; Anderson, R. A. J. Appl. Phys. 1978, 49, 1232.

(5) Scheinbeim, J. I.; Chung, K. T.; Pae, K. D.; Newman, B. A. J. Appl. Phys. 1979, 50, 6101.

(6) Takase, Y.; Tanaka, H.; Wang, T. T.; Caise, T.; Kometani, J. Macromolecules 1987, 20, 2318.

(7) Takase, Y.; Odajima, A.; Wang, T. T. J. Appl. Phys. 1986, 60, 2920.

(8) Wang, T. T. Ferroelectrics 1982, 41, 213.

(9) Furukawa, T.; Date, M.; Fukada, E. J. Appl. Phys. 1980, 51, 1135.

(10) Takahashi, N.; Odajima, A. Jpn. J. Appl. Phys. 1981, 20, L59.

(11) Takase, Y.; Odajima, A. Jpn. J. Appl. Phys. 1982, 21, L707.

(12) Furukawa, T.; Date, M.; Johnson, G. E. J. Appl. Phys. 1983, 54, 1540.

(13) Kaganov, M. I.; Omel'yanchun, A. N. Soviet Phys. JETP 1972, 34, 895.

(14) Binder, K.; Hohenberg, P. C. Phys. Rev. 1972, B6, 3461.

(15) Odajima, A.; Takase, Y.; Ishibashi, T.; Yuasa, K. Jpn. J. Appl. Phys. Supplement 1985, 24-2, 881.

(16) Wada, Y.; Hayakawa, R. Ferroelectrics 1981, 32, 115.

(17) Takahashi, N.; Odajima, A. Ferroelectrics 1981, 32, 49.

Figure captions

Figure 1. 1 (a): Diffractometer scans (reflection mode) at room temperature of five different samples of uniaxially oriented PVF_2 film; as-received, annealed at 120°C for 2 h, annealed then immersed in TCP at 100°C for 4 h, annealed then poled under 200 MV/m at 20°C, and annealed-doped then poled. 1 (b): Current densities vs electric field characteristics during the poling procedure of the last two samples. The period of the triangular shaped electric field was 640 s.

Figure 2. Current densities 2 (a) and electric displacements 2 (b) as a function of electric field when the PVF_2 film is subjected to triangular shape electric field with a period of 1000 s at 20°C. The dotted lines represent data for the doped film and the continuous line for the undoped film.

Figure 3. Depolarization current densities for the doped film 3 (a) and the undoped film 3 (b). Curves (1) - (4) represent the current densities for the films poled by a 1-min step pulse of 20, 60, 120 and 200 MV/m field strength, respectively, and curve (5) poled by sequential step pulses of 200 MV/m strength applied in opposite directions.

Figure 4. Depolarization current densities showing the polarization reversal process of the doped (dotted lines) and the undoped (continuous lines) films. Curves (1) and (2) represent characteristics of the films poled under +200 and -200 MV/m, respectively. Curves (3) and (4) represent characteristics of the film which are subjected to the poling sequence, E_p=+200 MV/m,

E_p=-200 MV/m followed by polarization reversal by applying field of E_p = +20 and +40 MV/m, respectively. Pulses of the poling field are also shown schematically and each step pulse width is 1 minute.

Figure 5. Pyroelectric coefficients in the cooling half cycle after heating up to 140°C of the doped films 5 (a) and of the undoped films 5 (b) as a function of temperature. Curves (1) - (5): poled by a step pulse of 20, 80, 120, 160 and 200 MV/m, respectively. Curve (6): poled by sequential step pulses of +200, -200 and +200 MV/m. Curve (7): poled by a pulse step sequence of +200 MV/m and -200 MV/m. Curve (8): poled by sequential step pulses of +200 MV/m, -200 and +20 MV/m. Curve (9): poled by sequential step pulses of +200 MV/m, -200 and +40 MV/m. Each step pulse width is 1 minute.

Figure 6. Polarization reversal process reflecting switching of thermally stable and unstable dipoles. Curve (1) is the trace of p_y as a function of reversal poling field at 40°C, a part of which is shown in Figure 5 (b). Curves (2) and (3) are the traces of the depolarization current densities as a function of reversal poling field (in Figure 4) at 135°C for doped and undoped samples, respectively.

Table I

2θ values and half widths, $\beta_{1/2}$, for the (110)(200) reflection for uniaxially oriented phase I PVF_2 films

sample	2θ, deg.	$\beta_{1/2}$, deg.
as-received	20.50	1.58
annealed	20.62	1.42
annealed and doped	20.64	1.36
annealed and poled	20.67	1.29
annealed, doped and poled	20.69	1.26

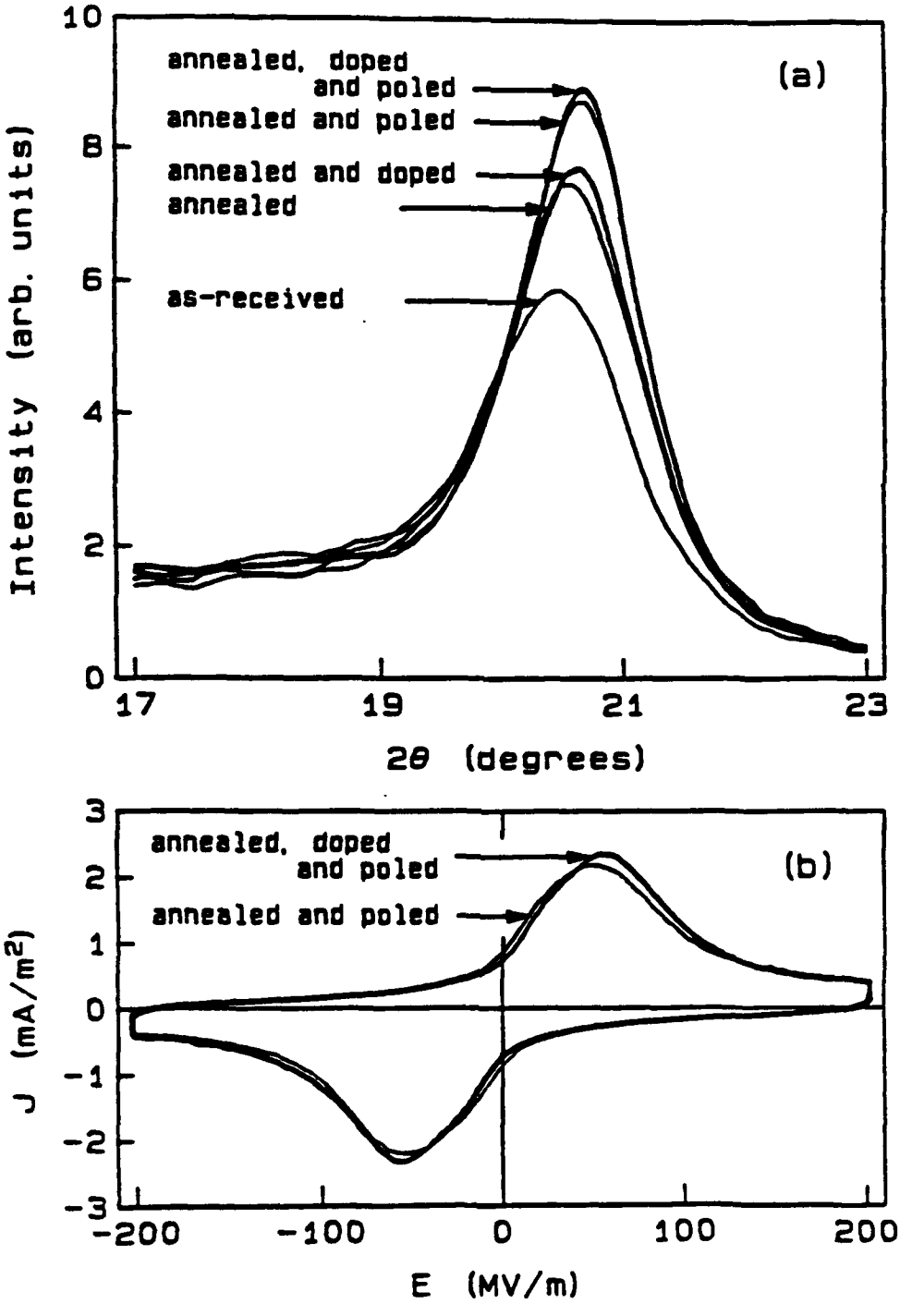
annealed, doped and poled
annealed and poled
annealed and doped
annealed
as-received
(a)
Intensity (arb. units)
2θ (degrees)
annealed, doped and poled
annealed and poled
(b)
J (mA/m²)
E (MV/m)

Fig. 1

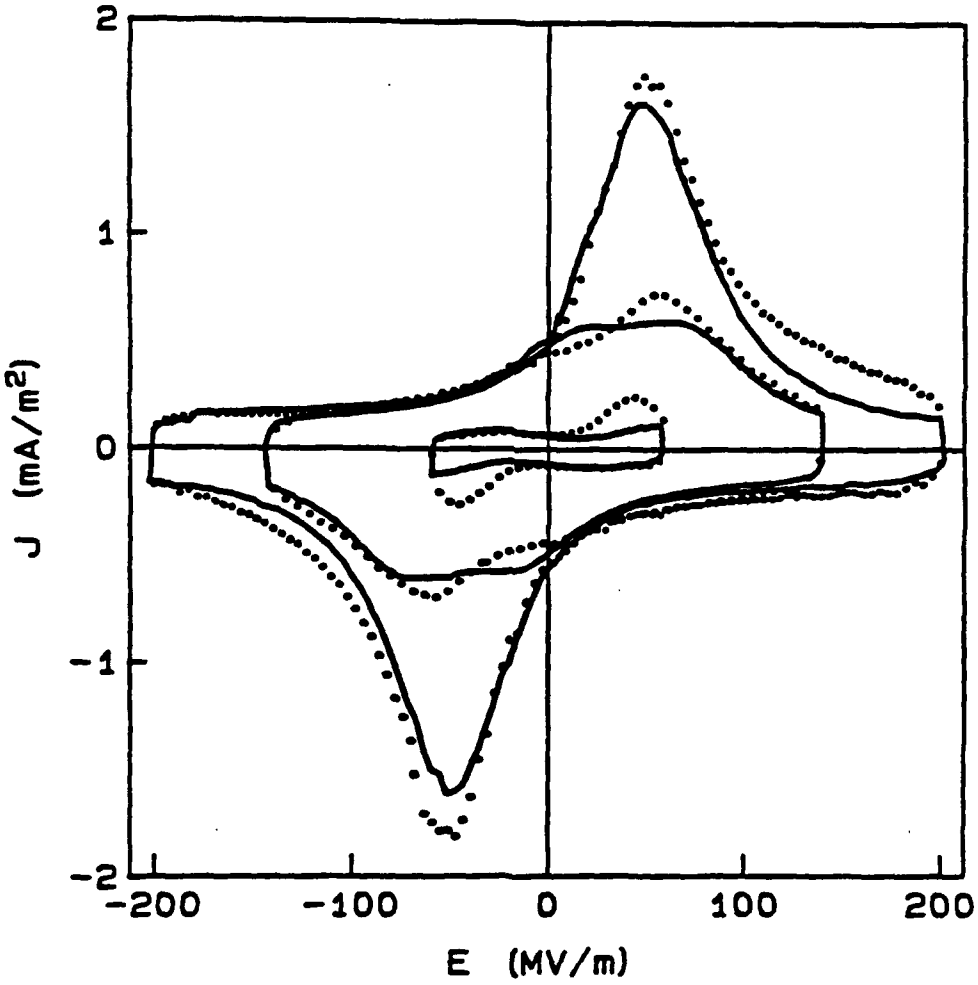

Fig. 2(a)

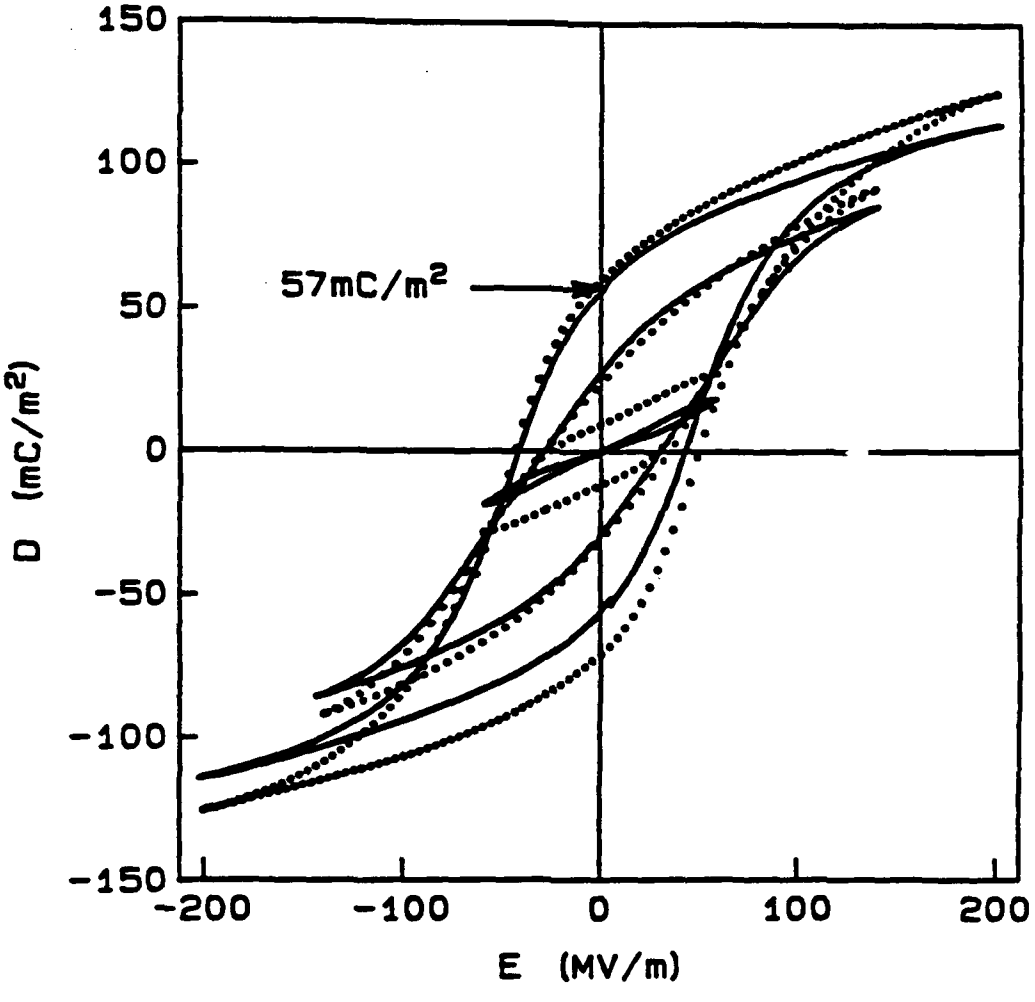

Fig. 2(b)

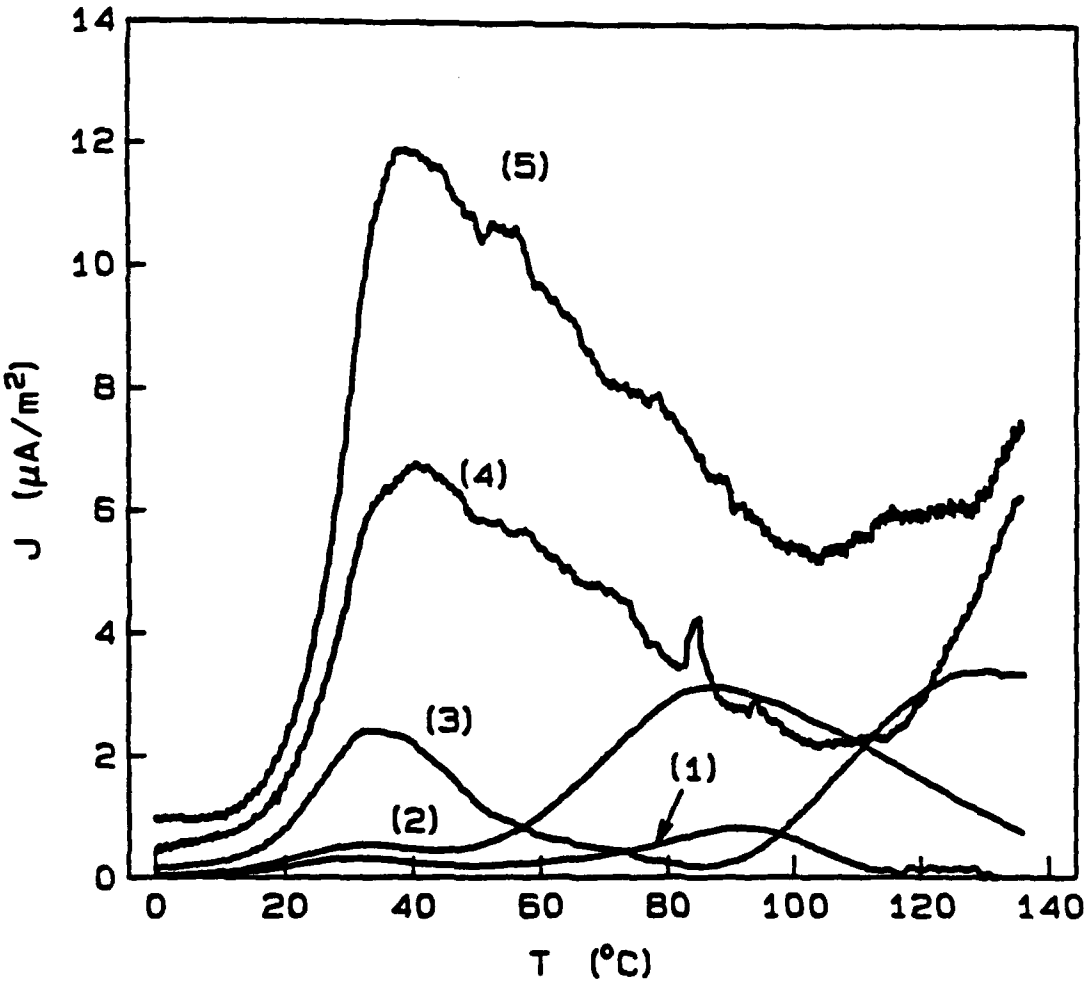

Fig. 3(a)

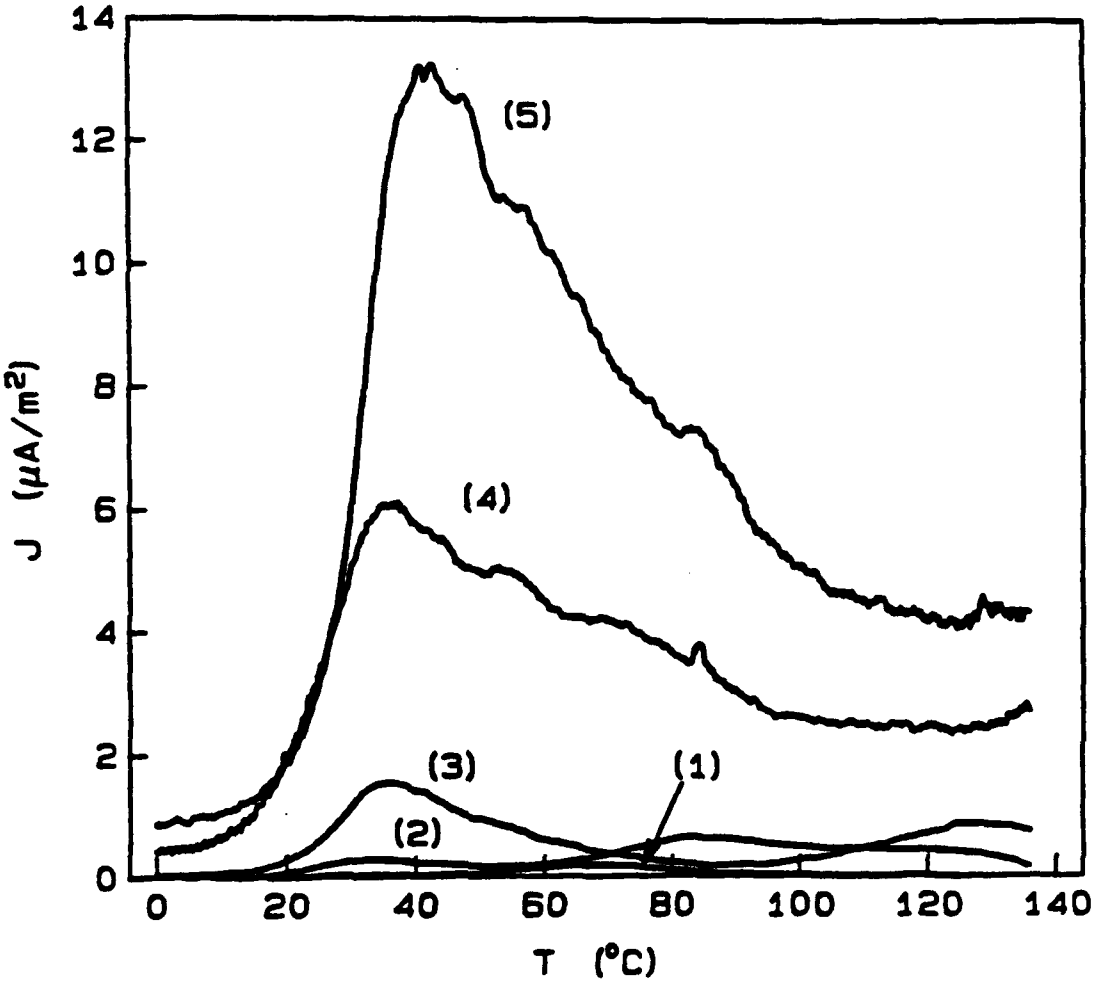

Fig. 3(b)

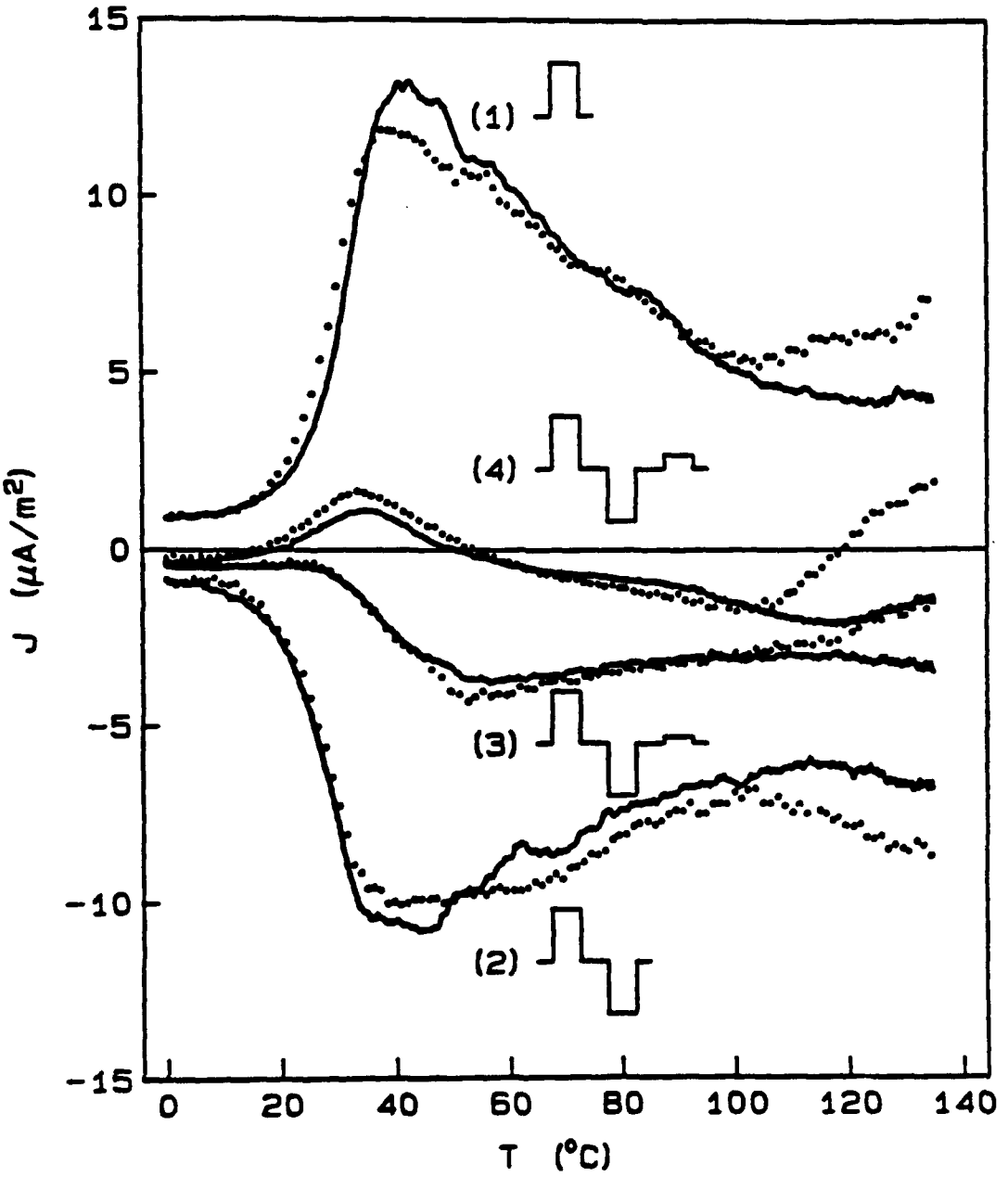

Fig. 4

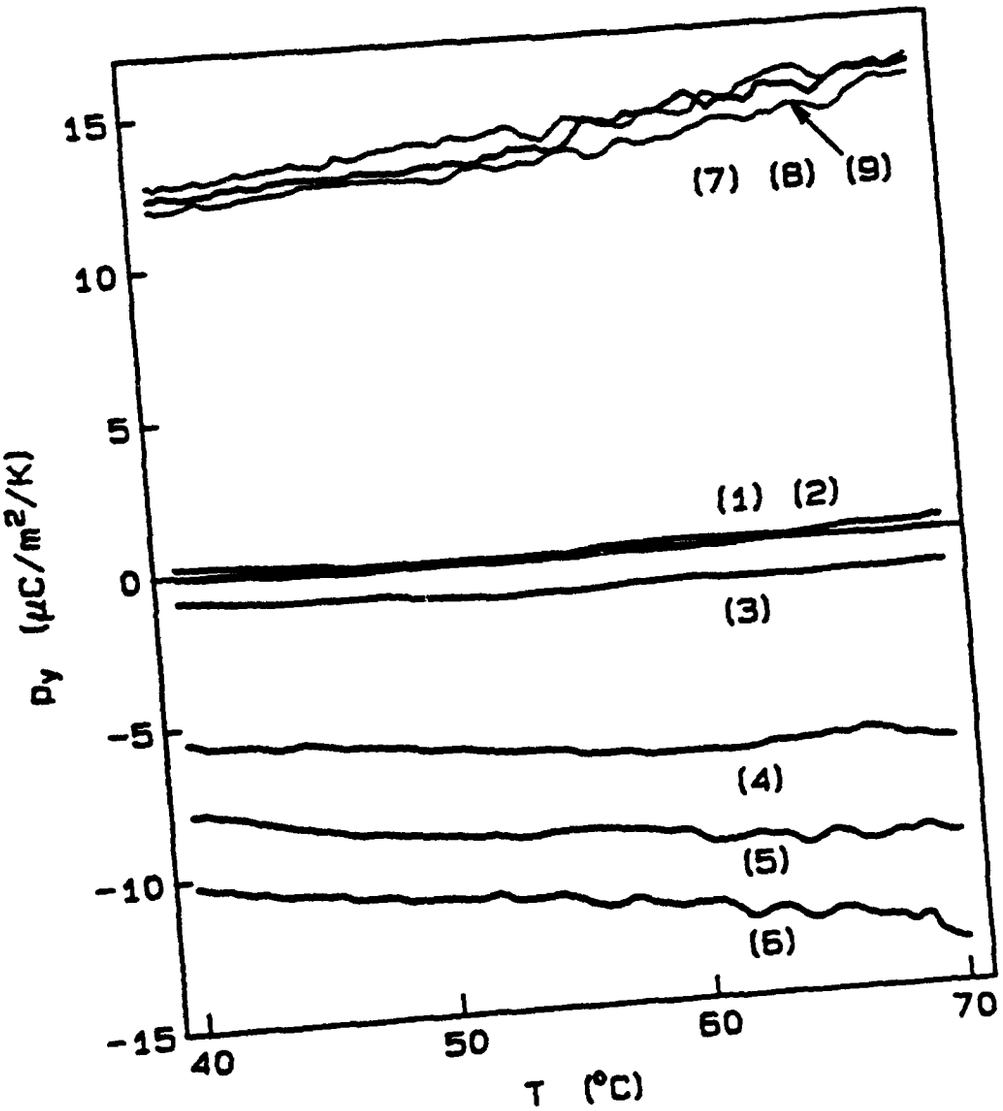

Fig. 5(a)

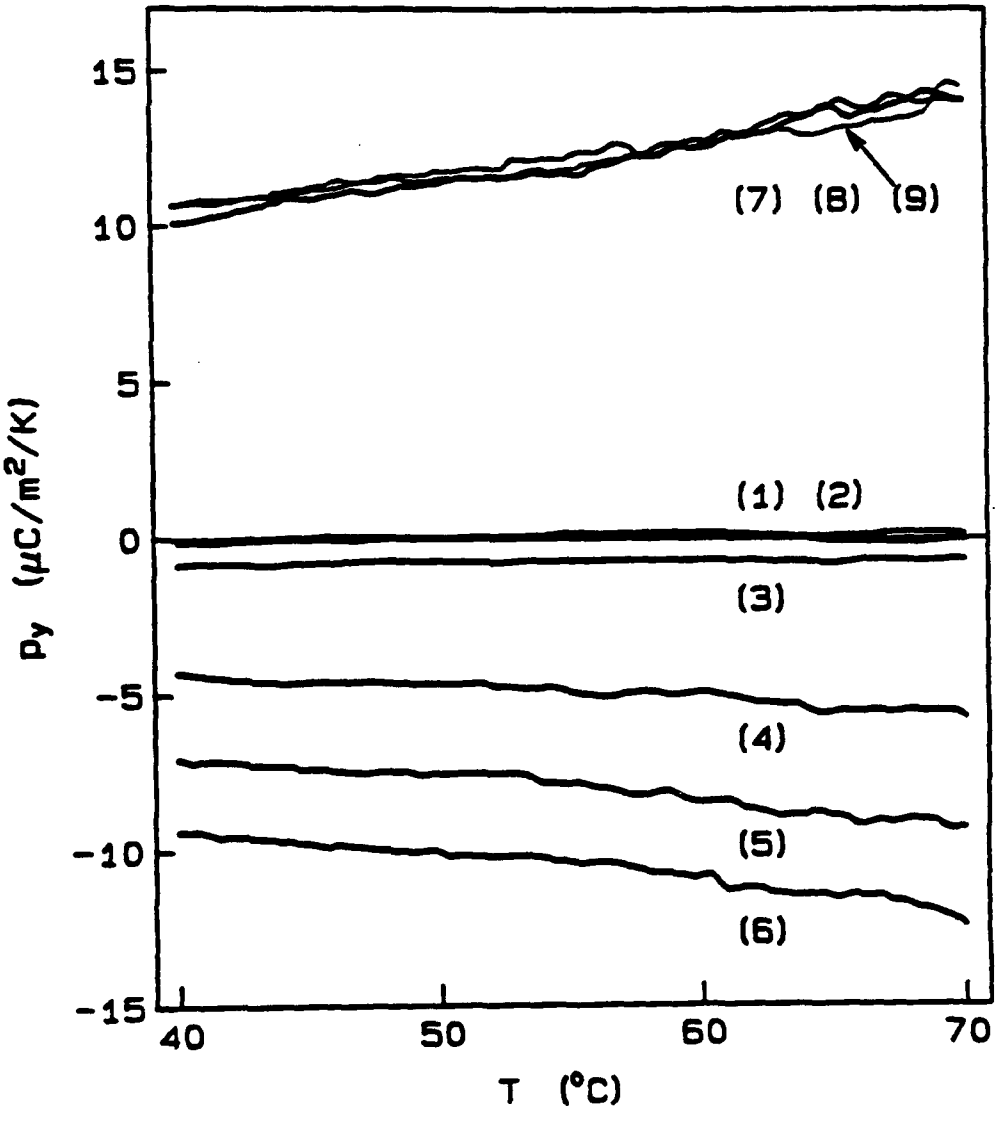

Fig. 5(b)

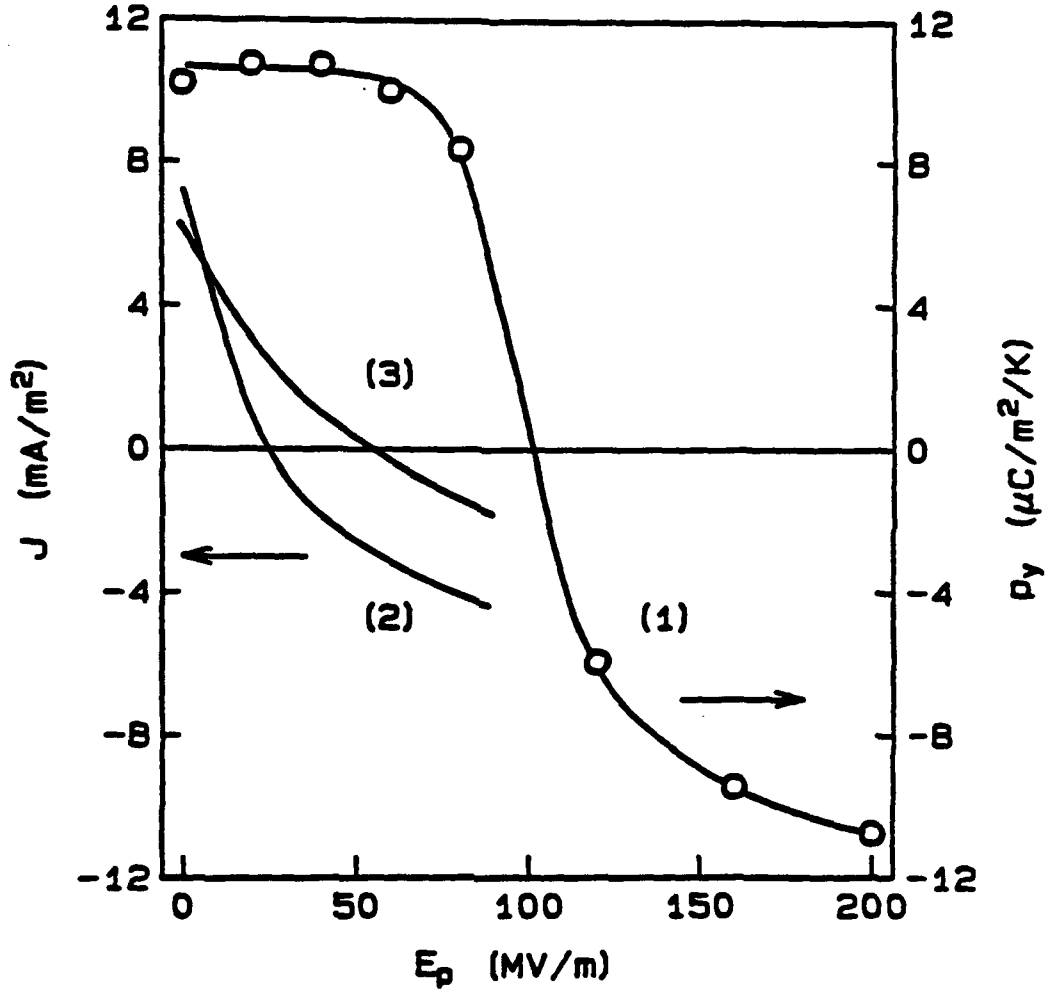

Fig. 6